4

Inviscid Flows and Potential Flow Theory

4.1 INTRODUCTION

The vorticity form of the Navier–Stokes Eq. (3.1.3) implies that if the flow of a fluid with constant density initially has zero vorticity, and the fluid viscosity is zero, then the flow is always irrotational. Such a flow is called an ideal, irrotational, or inviscid flow, and it has a nonzero velocity tangential to any solid surface. A real fluid, with nonzero viscosity, is subject to a no-slip boundary condition, and its velocity at a solid surface is identical to that of the solid surface.

As indicated in Sec. 3.4, in fluids with small kinematic viscosity, viscous effects are confined to thin layers close to solid surfaces. In Chap. 6, concerning boundary layers in hydrodynamics, viscous layers are shown to be thin when the Reynolds number of the viscous layer is small. This Reynolds number is defined using the characteristic velocity, U, of the free flow outside the viscous layer, and a characteristic length, L, associated with the variation of the velocity profile in the viscous layer. Therefore the domain can be divided into two regions: (a) the inner region of viscous rotational flow in which diffusion of vorticity is important, and (b) the outer region of irrotational flow. The outer region can be approximately simulated by a modeling approach ignoring the existence of the thin boundary layer and applying methods of solution relevant to nonviscous fluids and irrotational flows. Following the calculation of the outer region of irrotational flow, viscous flow calculations are used to represent the inner region, with solutions matching the solution of the outer region. However, in cases of phenomena associated with boundary layer separation, matching between the inner and outer regions cannot be done without the aid of experimental data.

The present chapter concerns the motion of inviscid, incompressible, and irrotational flows. In cases of such flows the velocity vector is derived from a

potential function. The vorticity of a vector derived from a potential function is zero, or

$$\vec{V} = \nabla\Phi \qquad \nabla \times \nabla\Phi = 0 \tag{4.1.1}$$

This expression indicates that every potential flow is also an irrotational flow.

In the following sections, special attention will be given to two-dimensional flows, which are the most common situation for analysis using potential flow theory. There also is some discussion of axisymmetric flows, and numerical solutions of two- and three-dimensional flows.

4.2 TWO-DIMENSIONAL FLOWS AND THE COMPLEX POTENTIAL

4.2.1 General Considerations

In cases of potential, incompressible, two-dimensional flows, velocity components are derived from the potential function, due to lack of vorticity, as well as from the stream function, due to the incompressibility of the fluid. Therefore the velocity components can be represented by

$$u = \frac{\partial\Phi}{\partial x} = \frac{\partial\Psi}{\partial y} \qquad v = \frac{\partial\Phi}{\partial y} = -\frac{\partial\Psi}{\partial x} \tag{4.2.1}$$

These relationships between the partial derivatives of the potential and stream functions are called the *Cauchy–Riemann equations*.

According to Eq. (4.2.1), the potential function can be determined by direct integration of the expressions for the velocity components,

$$\Phi = \int u\,dx + f(y) \qquad \text{or} \qquad \Phi = \int v\,dy + g(x) \tag{4.2.2}$$

The expression for $f(y)$ can be determined by

$$v = \frac{\partial}{\partial y}\left[\int u\,dx + f(y)\right] \Rightarrow \qquad f'(y) = v - \frac{\partial}{\partial y}\left[\int u\,dx\right] \Rightarrow$$

$$f(y) = \int \left\{ v - \frac{\partial}{\partial y}\left[\int u\,dx\right]\right\} dy \tag{4.2.3}$$

By the same approach, the expression for *g(x)* can be determined by

$$g(x) = \int \left\{ u - \frac{\partial}{\partial x}\left[\int v\,dy\right]\right\} dx \tag{4.2.4}$$

If the expression for the potential function is given, then the expression for the stream function can be obtained by applying Eq. (4.2.1). The

stream function expression also can be obtained by direct integration of the expressions of the velocity components, using

$$\Psi = -\int v\,dx + h(y) \quad \text{or} \quad \Psi = \int u\,dy + k(x) \tag{4.2.5}$$

where

$$\begin{aligned} h(y) &= \int \left\{ u + \frac{\partial}{\partial x}\left[\int v\,dy \right] \right\} dy \\ k(x) &= \int \left\{ v - \frac{\partial}{\partial x}\left[\int u\,dy \right] \right\} dx \end{aligned} \tag{4.2.6}$$

According to Eq. (4.1.1) the velocity vector is defined as the gradient of the function Φ. Therefore the velocity vector is perpendicular to the equipotential contour lines. According to Eq. (2.5.10), contour lines with a constant value of Ψ are streamlines, namely, lines that are tangential to the velocity vector. Therefore equipotential lines are perpendicular to the streamlines. A schematic of several streamlines and equipotential lines, called a *flow-net*, is presented in Fig. 4.1. The differences in value between each pair of adjacent streamlines is $\Delta\Psi$. The difference in value between each pair of adjacent

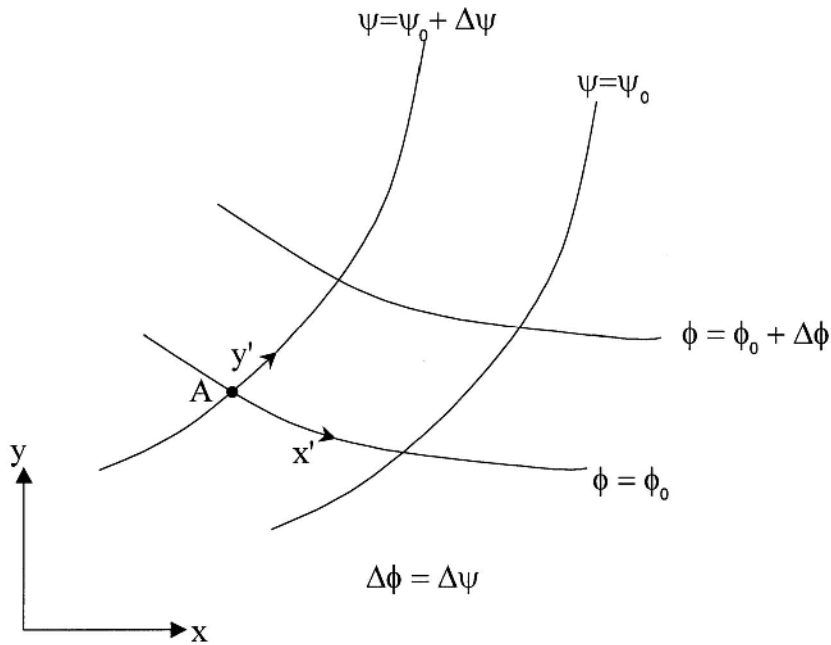

Figure 4.1 Schematics of a flow-net.

equipotential lines is $\Delta\Phi$. Usually, flow-nets are drawn so that $\Delta\Psi = \Delta\Phi$. Therefore, if at the point A of an intersection between a streamline and an equipotential line we adopt a Cartesian coordinate system, in which y' is tangential to the streamline and x' is tangential to the equipotential line, then according to Eq. (4.2.1), the small rectangle of the flow-net is a square.

By considering the incompressibility of the flow, as given by Eq. (2.5.7) or Eq. (2.5.8), and applying Eq. (4.1.1) or Eq. (4.2.1) with regard to the potential function, we obtain

$$\nabla \cdot (\nabla\Phi) = 0 \Rightarrow \qquad \nabla^2\Phi = 0 \Rightarrow \qquad \frac{\partial^2\Phi}{\partial x^2} + \frac{\partial^2\Phi}{\partial y^2} = 0 \tag{4.2.7}$$

This expression indicates that the potential function must satisfy the Laplace equation.

Consider now the irrotational flow condition, which is given by vanishing values of all components of vorticity, $\vec{\omega}$ in Eqs. (2.3.11) and (2.3.12), and apply Eq. (4.2.1) with regard to the stream function, so

$$\frac{\partial^2\Psi}{\partial x^2} + \frac{\partial^2\Psi}{\partial y^2} = 0 \tag{4.2.8}$$

indicating that the stream function also satisfies the Laplace equation. Therefore either the stream function or the potential function can be used for the presentation of the streamlines or equipotential lines.

If polar coordinates are used for the calculation of two-dimensional potential flow, then we may apply the following form of the Cauchy–Riemann equations,

$$u_r = \frac{\partial\Phi}{\partial r} = \frac{1}{r}\frac{\partial\Psi}{\partial\theta} \qquad v_\theta = \frac{1}{r}\frac{\partial\Phi}{\partial\theta} = -\frac{\partial\Psi}{\partial r} \tag{4.2.9}$$

where u_r and v_θ are components of the velocity vector in the r and θ directions, respectively. The potential and stream functions can be determined if expressions for the velocity components are given, according to the method represented by Eqs. (4.2.2)–(4.2.6).

The discussion in the previous paragraphs has indicated that equipotential lines (lines of constant value of Φ) are orthogonal to streamlines (lines of constant value of Ψ). Therefore it is possible to consider the complex function w, as given by Eq. (1.3.91), which incorporates both functions in the complex domain. We may consider the plane w, which is depicted by the coordinates Φ and Ψ, as shown in Fig. 4.2. Equipotential lines and streamlines in the w plane of that figure represent the schematic of the flow-net. The plane of the complex variable z is depicted by applying the coordinates x and y. Streamlines and equipotential lines depicted in the z plane represent the common flow-net. The transformation of $\Phi-\Psi$ mapping in the w plane to $x-y$ mapping in the

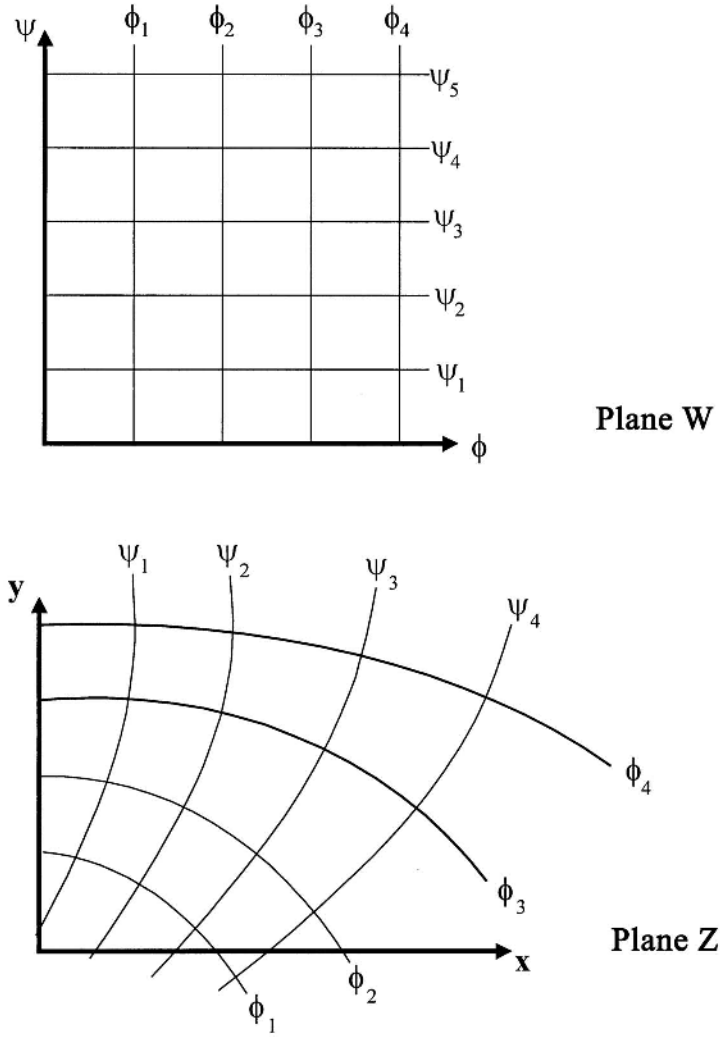

Figure 4.2 An example of conformal mapping.

z plane is called *conformal mapping*. An example of conformal mapping is represented in Fig. 4.2. Small squares in the w plane are transformed into small squares in the z plane by this procedure. The function w is called *the complex potential* and is represented by

$$w = \Phi + i\Psi \tag{4.2.10}$$

The major properties of the complex potential and its implications with regard to Ψ and Φ are presented in Eqs. (1.3.90)–(1.3.99). The complex potential function is an analytical function, namely, a function of z. Various functions of z can be useful for the description and depiction of different flow domains, in terms of equipotential lines and streamlines.

As shown by Eqs. (4.2.7) and (4.2.8), the potential function and stream function satisfy the Laplace equation. Therefore the complex potential function also satisfies the Laplace equation, as it represents a linear combination of Φ and Ψ. Also, the Laplace equation is a linear differential equation. Therefore, if the complex potential w_1 represents a potential flow domain, and w_2 represents another potential flow domain, then any linear combination such as $\alpha w_1 + \beta w_2$ also represents a potential flow domain.

As shown by Eqs. (1.3.92)–(1.3.97),

$$\frac{dw}{dz} = \frac{\partial w}{\partial x} = -i\frac{\partial w}{\partial y} = \frac{\partial \Phi}{\partial x} + i\frac{\partial \Psi}{\partial x} = u - iv = \tilde{V} \tag{4.2.11}$$

This expression indicates that the derivative of w is equal to the conjugate of the velocity.

One further point to note is that, in a potential flow domain, the Bernoulli equation is satisfied between any two points of reference, as shown by Eqs. (2.6.10)–(2.6.12). This provides an important tool for analyzing pressure distributions in potential flows, as will be seen in the following subsections, where we review several special cases of two-dimensional potential flows.

4.2.2 Uniform Flow

Consider a flow with constant speed U, parallel to the x coordinate. This might represent, for example, the flow of air above the earth. Components of the velocity vector are then given by

$$u = U \qquad v = 0 \tag{4.2.12}$$

By applying Eqs. (4.2.2)–(4.2.6), we obtain

$$\Phi = Ux \qquad \Psi = Uy \qquad w = U(x + iy) = Uz \tag{4.2.13}$$

These expressions indicate that streamlines are parallel horizontal lines. For each streamline, the value of the y coordinate is constant. Equipotential lines are vertical lines. For each equipotential line the value of the x coordinate is kept constant. Also, according to the Bernoulli equation (2.6.12), the pressure is constant along horizontal streamlines and varies as hydrostatic pressure in the vertical direction.

If the parallel flow streamlines make an angle α with respect to the x coordinate, then the complex potential is given by

$$w = Uz\,e^{-i\alpha} \tag{4.2.14}$$

4.2.3 Flow at a Corner

Consider the flow domain represented by the complex potential function

$$w = Az^2 = A\left[(x^2 - y^2) + i2xy\right] \tag{4.2.15}$$

where A is a constant positive coefficient. The conjugate velocity is given by

$$\tilde{V} = u - iv = \frac{dw}{dz} = 2Az = 2A(x + iy) \tag{4.2.16}$$

Equations (4.2.15) and (4.2.16) imply

$$\Phi = A(x^2 - y^2) \qquad \Psi = 2Axy \qquad u = 2Ax \qquad v = -2Ay \tag{4.2.17}$$

Therefore equipotential lines and streamlines are hyperbolas, as shown in Fig. 4.3. On the streamlines, small arrows show the flow direction. They are depicted according to signs of the velocity components implied by Eq. (4.2.17). This equation indicates that the velocity vanishes at the coordinate origin. Therefore this point is a singular stagnation point. At a singular point, the velocity vanishes or becomes infinite. If the velocity vanishes, the point is a stagnation point. If the velocity has infinite value, it is a cavitation point. Streamlines or equipotential lines may intersect only at singular points. Eq. (4.2.17) also indicates that the velocity increases with distance from the origin. However, there is no particular singular point of infinite velocity.

By employing the Bernoulli equation, the distribution of pressure along the x coordinate is

$$p = p_0 - 2\rho A^2 x^2 \tag{4.2.18}$$

where p_0 is the pressure at the origin. In Fig. 4.3, a parabolic curve shows the pressure distribution along the x-direction. It indicates that the flow at the corner cannot persist for large distances from the origin, since according to Eq. (4.2.18), at some distance from the origin the pressure is too low to afford the streamline pattern of Eq. (4.2.17).

If the flow takes place at a corner of angle $\alpha = \pi/n$, then the complex potential is given by

$$w = Az^n \tag{4.2.19}$$

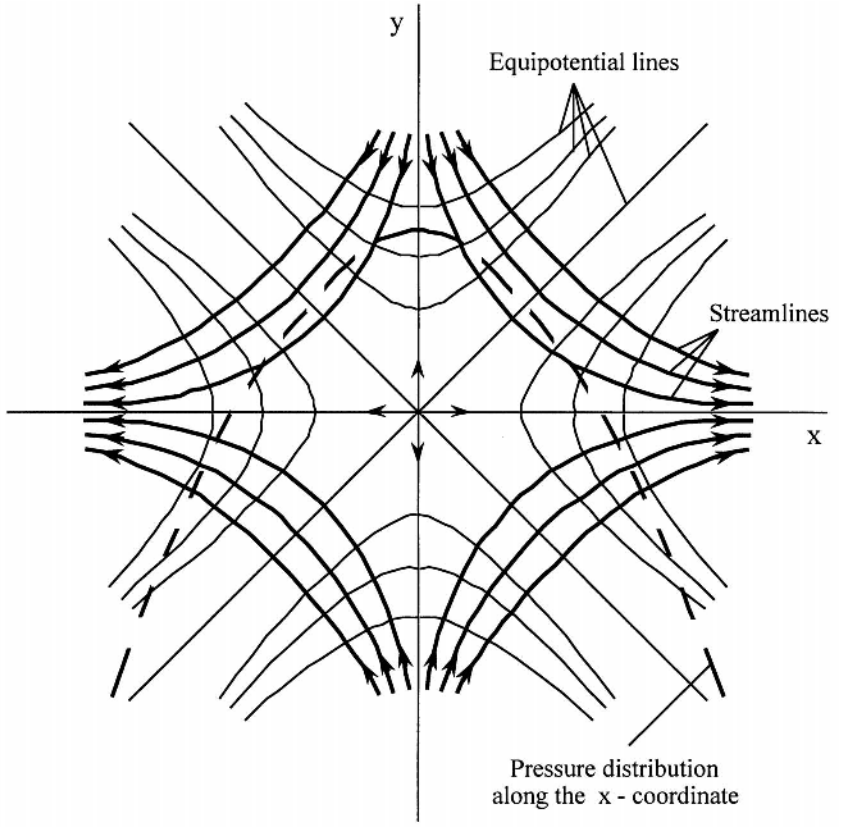

Figure 4.3 Flow at a 90° corner.

4.2.4 Source Flow

The complex potential function for a source flow is

$$w = \frac{q}{2\pi} \ln z = \frac{q}{2\pi} \ln(r\, e^{i\theta}) = \frac{q}{2\pi}(\ln r + i\theta) \tag{4.2.20}$$

Therefore the potential and stream functions are given, respectively, by

$$\Phi = \frac{q}{2\pi} \ln r \qquad \Psi = \frac{q}{2\pi}\theta \tag{4.2.21}$$

These expressions indicate that streamlines are straight lines radiating outward from the origin. For each streamline, the value of Ψ is kept constant. Equipotential lines are concentric circles surrounding the coordinate origin. For each equipotential line, the value of r is kept constant.

It is possible to use the expressions for the potential function, the stream function, or the complex potential function for the calculation of the velocity components. We exemplify here application of the complex potential function:

$$\tilde{V} = u - iv = \frac{dw}{dz} = \frac{q}{2\pi z} = \frac{q\tilde{z}}{2\pi z\tilde{z}} = \frac{q}{2\pi}\left(\frac{x - iy}{x^2 + y^2}\right) \tag{4.2.22}$$

Therefore the complex velocity is given by

$$V = \frac{q}{2\pi}\left(\frac{x + iy}{x^2 + y^2}\right) = \frac{q}{2\pi}\left(\frac{\cos\theta + i\sin\theta}{r}\right) = \frac{q}{2\pi r}e^{i\theta} \tag{4.2.23}$$

This result indicates that the absolute velocity is kept constant in a circle surrounding the origin, i.e., the fluid flows in the radial direction. The velocity is infinite at the origin and vanishes at a large distance from the origin.

If a circle of radius r is drawn around the coordinate origin, then the radial flow velocity of the fluid that penetrates the circle is given by

$$V = u_r = \frac{q}{2\pi r} \tag{4.2.24}$$

It should be noted that the complex velocity of Eq. (4.2.23) is different from the absolute velocity of Eq. (4.2.24). Equation (4.2.24) indicates that the source strength q represents the total flow rate penetrating the circle surrounding the origin.

If the flow domain is horizontal, then Bernoulli's equation yields

$$p = p_\infty - \rho\frac{V^2}{2} = p_\infty - \frac{\rho}{2}\left(\frac{q}{2\pi}\right)^2\frac{1}{r^2} \tag{4.2.25}$$

where p_∞ is the pressure at an infinite distance from the source point. At the origin the pressure is infinitely negative. Therefore the origin is a singular cavitation point.

Figure 4.4 shows the flow-net and pressure distribution along a radial coordinate of a source flow.

4.2.5 Simple Vortex

We consider the flow domain represented by the complex potential,

$$w = -\frac{i\kappa}{2\pi}\ln z = \frac{\kappa}{2\pi}(\theta - i\ln r) \tag{4.2.26}$$

According to this expression,

$$\Phi = \frac{\kappa}{2\pi}\theta \qquad \Psi = -\frac{\kappa}{2\pi}\ln r \tag{4.2.27}$$

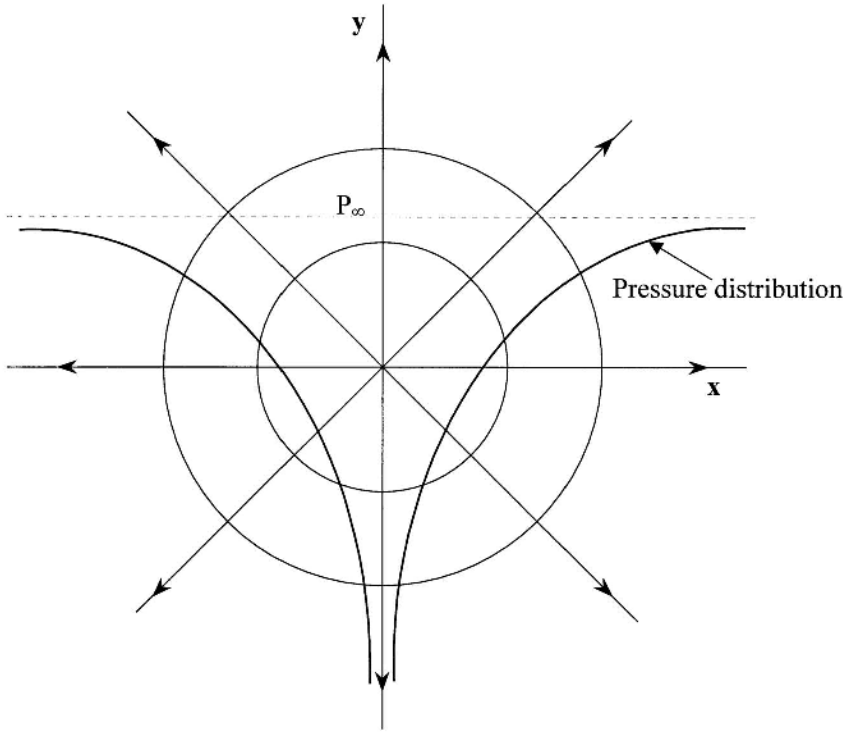

Figure 4.4 Source of flow.

These relations indicate that equipotential lines are straight radial lines emanating from the coordinate origin, while streamlines are circles surrounding the origin.

By appropriate differentiation of either of the expressions given by Eq. (4.2.27), expressions for the velocity components may be obtained as

$$u_r = 0 \qquad v_\theta = \frac{\kappa}{2\pi r} \tag{4.2.28}$$

These expressions indicate that the velocity is proportional to the inverse of the distance from the coordinate origin, its value is constant along circles surrounding the origin, and its direction is counterclockwise. At the origin, the velocity is infinite. Therefore this point is a singular cavitation point. The pressure distribution along a radial coordinate is identical to that given by Eq. (4.2.25) for the source flow, where κ replaces q. Figure 4.5 shows the flow-net and pressure distribution along a radial coordinate of a simple vortex flow.

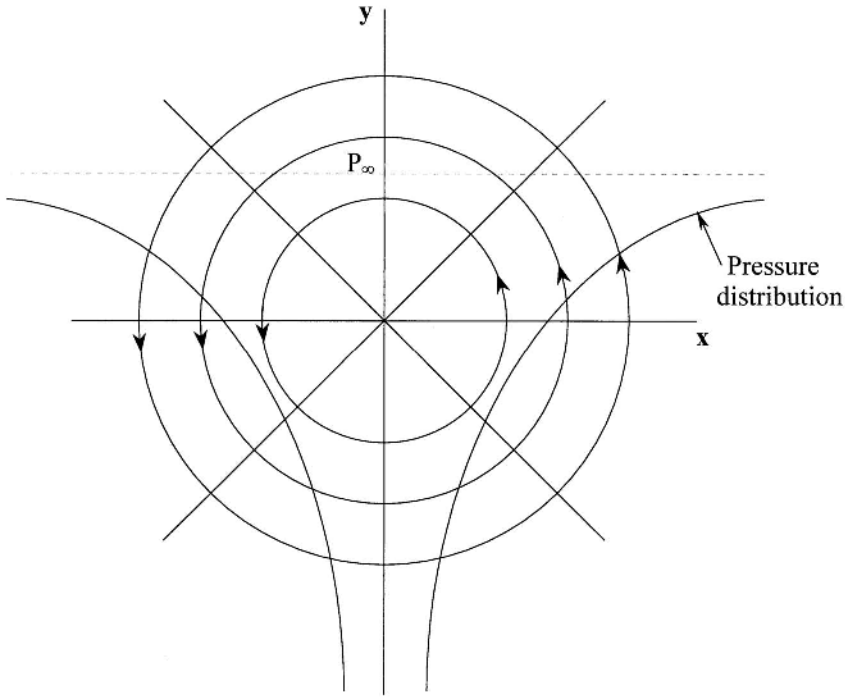

Figure 4.5 Simple vortex.

If we depict a circle of radius r about the origin and calculate the circulation by the integral of Eq. (2.3.14), we obtain

$$\Gamma = \oint \vec{V} \cdot d\vec{s} = \int_0^{2\pi} v_\theta r \, d\theta = \int_0^{2\pi} \frac{\kappa}{2\pi r} r \, d\theta = \kappa \tag{4.2.29}$$

This expression indicates that κ represents the circulation of the vortex, namely, the *vortex strength*. According to Eq. (2.3.15), the circulation is zero for a potential flow domain. However, if in a potential flow domain the closed curve of the integral of Eq. (2.3.14) surrounds singular points of circulating flows, then the circulation does not vanish. It represents the strength of the circulating flow, in the domain surrounding that singular point.

4.2.6 Doublet

Doublet flow is obtained due to the superposition of a positive and a negative source of equal strength. The distance between the sources is a, the strength of

each source is q, and the following conditions take place in the flow domain:

$$\begin{aligned} a &\to 0 \\ q &\to \infty \\ \frac{aq}{\pi} &\to \lambda \end{aligned} \tag{4.2.29}$$

The complex potential function of the doublet is developed as follows:

$$\begin{aligned} w &= \frac{q}{2\pi} \ln\left[\frac{z+a}{z-a}\right] = \frac{q}{2\pi} \ln\left[\frac{z^2+2az+a^2}{z^2-a^2}\right] \\ &= \frac{q}{2\pi} \ln\left[\frac{1+(2a/z)}{1-(a/z)^2} + \frac{a^2}{z^2-a^2}\right] \\ w &\to \frac{q}{2\pi} \ln\left[\left(1+\frac{2a}{z}\right)\left(1+\frac{a^2}{z^2}\ldots\right)\right] \to \frac{q}{2\pi}\frac{2a}{z} = \frac{\lambda}{z} \end{aligned} \tag{4.2.30}$$

The doublet of Eq. (4.2.30) incorporates a positive source, located to the left of the origin (at $x = -a$), and a negative source, located to the right of the origin (at $x = a$).

According to Eq. (4.2.30), we can find the potential and stream functions as follows:

$$w = \Phi + i\Psi = \frac{\lambda}{z} = \frac{\lambda}{r}e^{-i\theta} = \frac{\lambda}{r}(\cos\theta - i\sin\theta) \tag{4.2.31}$$

Therefore

$$\Phi = \frac{\lambda\cos\theta}{r} = \frac{\lambda x}{x^2+y^2} \qquad \Psi = -\frac{\lambda y}{x^2+y^2} \tag{4.2.32}$$

The equation of equipotential lines is

$$\left(x - \frac{\lambda}{2\Phi}\right)^2 + y^2 = \left(\frac{\lambda}{2\Phi}\right)^2 \tag{4.2.33}$$

This expression indicates that equipotential lines are circles, which pass through the origin, and have their centers located on the x axis. By applying the expression for Ψ in Eq. (4.2.32), the equation for the streamlines is

$$x^2 + \left(y + \frac{\lambda}{2\Psi}\right)^2 = \left(\frac{\lambda}{2\Psi}\right)^2 \tag{4.2.34}$$

This expression indicates that streamlines are circles, passing through the origin, whose centers are located on the y axis.

The conjugate velocity is obtained by differentiating Eq. (4.2.31) to obtain

$$\tilde{V} = -\frac{\lambda}{z^2} = -\frac{\lambda}{r^2}e^{-2i\theta} = \frac{\lambda}{r^2}[-\cos(2\theta) + i\sin(2\theta)] \tag{4.2.35}$$

Therefore components of the velocity are given by

$$u = -\frac{\lambda}{r^2}\cos(2\theta) = -\frac{\lambda}{x^2+y^2}\left(\frac{x^2-y^2}{x^2+y^2}\right) = \frac{\lambda(y^2-x^2)}{(x^2+y^2)^2}$$
$$v = -\frac{\lambda}{r^2}\sin(2\theta) = -\frac{\lambda}{x^2+y^2}\left(\frac{2xy}{x^2+y^2}\right) = -\frac{2\lambda xy}{(x^2+y^2)^2} \tag{4.2.36}$$

The flow net for a doublet is sketched in Fig. 4.6.

4.2.7 The Image Method

The flow domain given by the potential, stream, and complex potential functions is basically infinite. Considerations of solid boundaries in such a domain are usually made by assuming that solid boundaries are represented by particular streamlines (note that there is no flow *across* a streamline). Representation of solid boundaries by particular streamlines often requires the superposition of several simple potential flows. The presentation of flow around a cylinder,

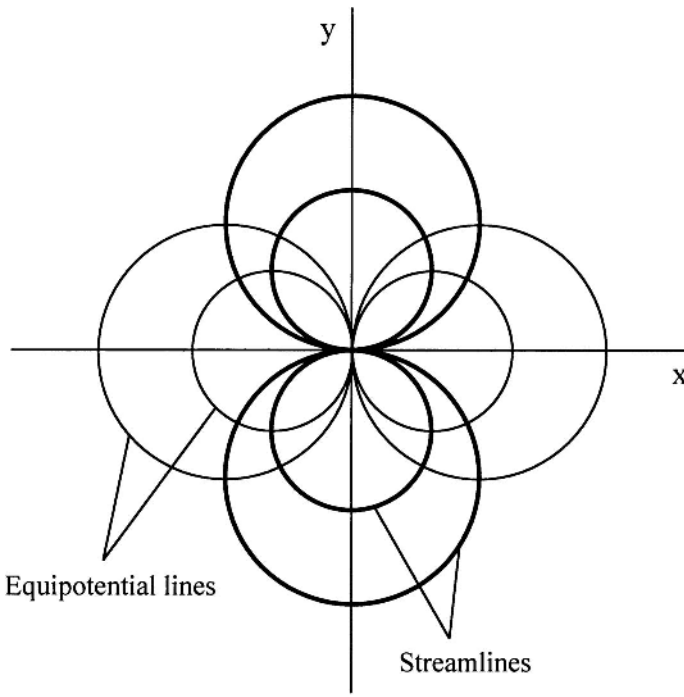

Figure 4.6 Flow associated with a doublet.

as shown in Sec. 4.5, is obtained by the superposition of a uniform flow and a doublet flow. Very often, adequate superposition is obtained by trial-and-error experiments, but in some particular cases the appropriate superposition is obtained by straightforward calculations.

Figure 4.7 shows a source located at a distance $x = a$ from a solid wall. There is no flow perpendicular to the wall. Therefore to obtain a velocity tangential to the wall at point A, a second source must be added, of identical strength, at $x = -a$. The complex potential describing the flow created by a source of strength q, located at a distance a from a wall, is given by

$$w = \frac{q}{2\pi} \ln[(z - a)(z + a)] \tag{4.2.36}$$

Figure 4.8 shows a source located at a corner between two solid walls. The distance of the source from one wall is $x = a$. The distance from the other wall is $y = b$. In this case, to represent the two walls as streamlines, the superposition should incorporate four sources, as indicated by Fig. 4.8.

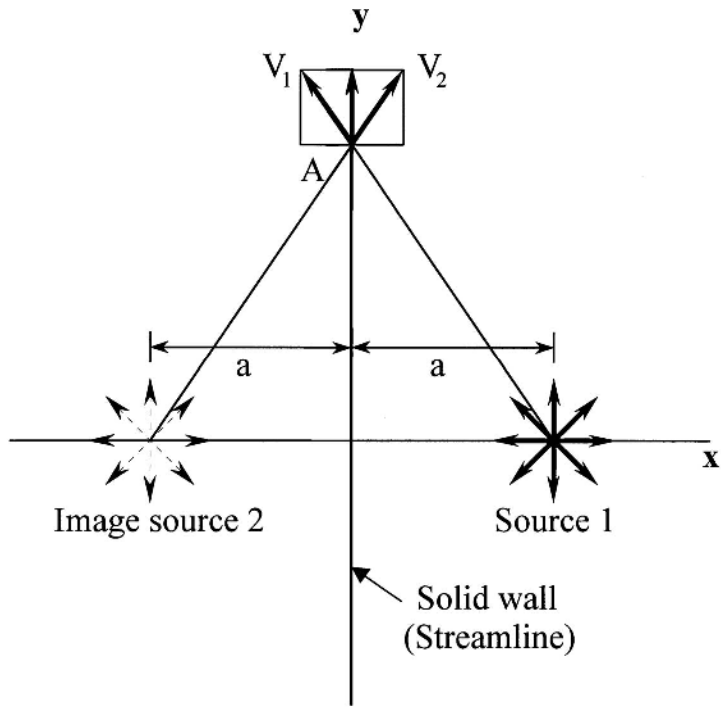

Figure 4.7 Source located at a wall.

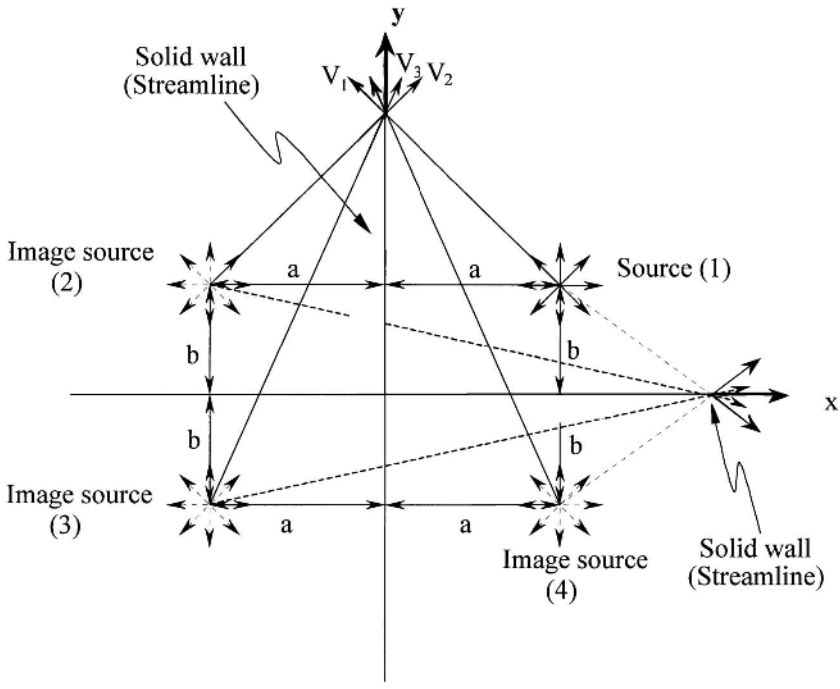

Figure 4.8 Source at the corner between two walls.

Therefore the complex potential function is given by

$$w = \frac{q}{2\pi} \ln[(z - a - ib)(z + a - ib)(z + a + ib)(z - a + ib)] \quad (4.2.37)$$

Figure 4.9 shows a source of strength q located at a distance $x = a$ from an equipotential straight line given by $x = 0$. Practically, such a case can be useful for the calculation of groundwater flow at an injection well, which is located close to a river. Section 4.3 provides details concerning the application of the potential flow theory to calculations of flow through porous media. To keep the line $x = 0$ as an equipotential line, another negative source of equal strength should be added at $x = -a$, as shown in Fig. 4.9. Therefore the complex potential function is given by

$$w = \frac{q}{2\pi} \ln\left(\frac{z - a}{z + a}\right) \quad (4.2.38)$$

Figure 4.10 shows a vortex of circulation κ, located at the corner between two solid walls, given by $x = 0$ and $y = 0$. Its distance from one wall is $x = a$,

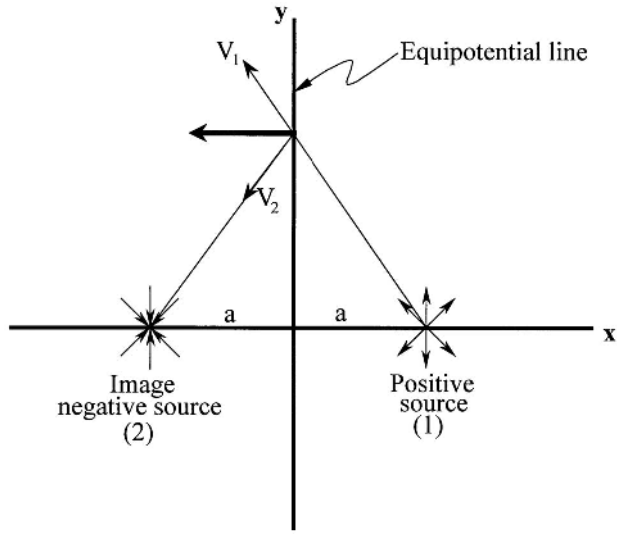

Figure 4.9 Source at an equipotential line.

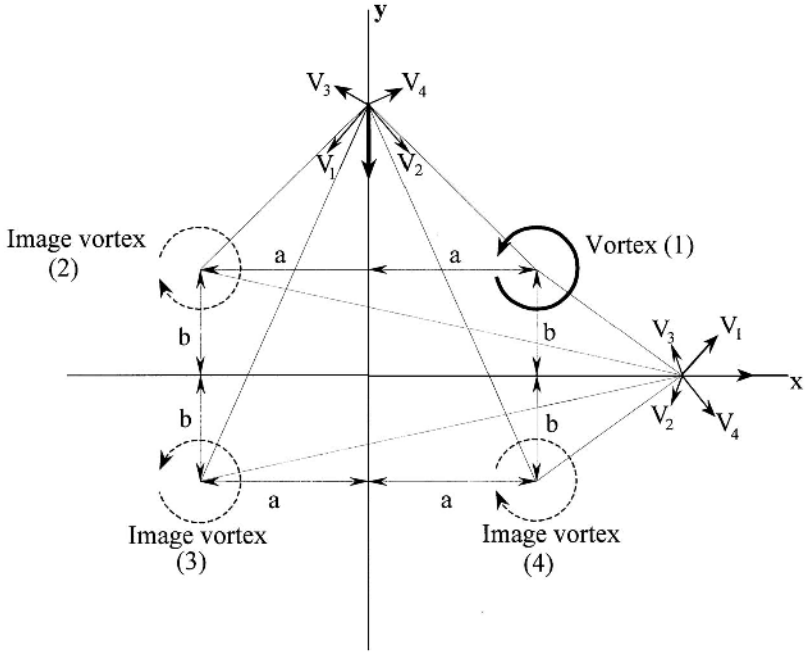

Figure 4.10 Vortex at the corner between two solid walls.

and its distance from the other wall is $y = b$. To represent the lines $x = 0$ and $y = 0$ as streamlines, three vortices of equal circulation should be added, as shown in Fig. 4.10. Therefore the complex potential function is given by

$$w = -\frac{i\kappa}{2\pi} \ln \left[\frac{(z - a - ib)(z + a + ib)}{(z + a - ib)(z - a + ib)} \right] \tag{4.2.40}$$

It should be noted that for relevance to real-world problems, positive and negative sources are kept in a stable position, whereas the vortex of Fig. 4.10 is subject to movement in the domain. The position change of the vortex of this figure is caused by the flow velocity components of the image vortices.

4.3 FLOW THROUGH POROUS MEDIA

Flow through porous media such as aquifers, alluvial material, sand, small gravel, etc. is usually laminar flow, associated with very small Reynolds numbers. The definition of the Reynolds number for flow through porous media is

$$\mathrm{Re} = \frac{q d_p}{\nu} \tag{4.3.1}$$

where q is the specific discharge (with dimensions of LT^{-1}); d_p is a characteristic pore size, usually considered as a representative average diameter of the particles comprising the matrix, or derived from the permeability (another concept that will be defined later) of the porous matrix, and ν is the kinematic viscosity of the fluid. The specific discharge, called also filtration velocity, is related to the average interstitial flow velocity by

$$q = V\phi \tag{4.3.2}$$

where ϕ is the porosity of the matrix. In an isotropic material the volumetric and surface porosity are identical. It should be noted that V represents the velocity of advection of contaminants migrating with the flowing fluid through the porous matrix. The quantity q represents the flow rate per unit surface of the porous matrix.

In most cases of environmental flow through porous media, the value of the Reynolds number, defined in eq. (4.3.1), is smaller than unity. Therefore flow through porous media in most cases may be considered as laminar creeping flow (Section 3.3). However, there are also examples in which the Reynolds number is higher, as with flows through coarse gravel, flows through rock fill, wave breakers, etc. The present section refers only to creeping flow through porous media; other topics in porous media flow are discussed in Chap. 11.

In creeping flows, the equations of motion (Navier–Stokes) reduce to

$$\nabla p' = \mu \nabla^2 \vec{V} \tag{4.3.3}$$

where $p = \rho g$ is the piezometric pressure, V is the flow velocity, and μ is the viscosity of the fluid.

4.3.1 Darcy's Law

The laminar flow through a porous matrix can be visualized as a flow through many parallel flat plates, or through a bundle of capillaries. With regard to a single capillary of diameter d and length L, we may apply the solution of Poiseuille–Hagen to Eq. (4.3.3) to obtain

$$J = \frac{\Delta h}{L} = \frac{1}{\rho g} \frac{\Delta p^*}{L} = \frac{32v}{gd^2} V \tag{4.3.4}$$

where h is the piezometric head and J is the hydraulic gradient. The capillary diameter, d, may be considered as a characteristic pore size of the porous matrix.

Considering that the porosity, ϕ, represents the ratio between the total area of cross sections of the bundle of capillaries and the cross section of the porous matrix, Eq. (4.3.4) implies

$$q = KJ \tag{4.3.5}$$

where K is the hydraulic conductivity of the porous matrix, given by

$$K = \frac{gd^2\phi}{32v} \tag{4.3.6}$$

This result shows that the hydraulic conductivity depends on properties of the porous matrix, namely the porosity, the characteristic pore size, and also the kinematic viscosity of the fluid. The permeability is a parameter associated with the flow through the porous matrix and depends solely on the matrix properties. Its definition and relation to the hydraulic conductivity are given as

$$k = \frac{\phi d^2}{32} \qquad K = \frac{gk}{v} \tag{4.3.7}$$

For three-dimensional domains, Eq. (4.3.5) can be generalized as

$$\vec{q} = -K \nabla h \tag{4.3.8}$$

This proportionality between the specific discharge and the gradient of the piezometric head is called *Darcy's law*.

4.3.2 Relevance of Potential Flow Theory

Equation (4.3.8) implies that, in cases of constant hydraulic conductivity, the specific discharge vector originates from a gradient of a potential function Φ, which is equal to Kh. In cases of two-dimensional flow, with negligible compression of the fluid and the solid matrix, it is possible to define a stream function, Ψ, that satisfies continuity and has constant values along the streamlines. The relationships between the components of the specific discharge and the functions Φ and Ψ are

$$\begin{aligned} q_x &= -\frac{\partial \Phi}{\partial x} = -\frac{\partial \Psi}{\partial y} \\ q_x &= -\frac{\partial \Phi}{\partial y} = \frac{\partial \Psi}{\partial x} \end{aligned} \tag{4.3.9}$$

The negative sign for the derivatives in Φ shows that the flow is in the direction of decreasing values of Φ. These relations are basically Cauchy–Riemann equations, as introduced earlier in Sec. 4.2.1. The continuity, represented by Ψ, and the potential function Φ, both satisfy the Laplace equation,

$$\nabla^2 \Phi = 0 \qquad \nabla^2 \Psi = 0 \qquad \nabla^2 h = 0 \tag{4.3.10}$$

Therefore all techniques applicable to the solution of the Laplace equation can be used for the calculation of incompressible flow through porous media. The function theory with the employment of complex variables is useful for the evaluation of practical issues associated with flow through porous media. In potential fluid flows, the potential function has no physical meaning. In flow through porous media, the potential function, Φ, is derived from the piezometric head.

On the basis of Eq. (4.3.9), flow-nets can often be defined to obtain quick estimates of the intensity of the flow through a limited-size porous medium. They also can easily provide estimates of uplift forces exerted on structures. The flow-net incorporates a grid of small squares whose boundaries are equipotential lines and streamlines, as noted previously. Calculations of uplift forces and total flow through the domain are based on the number of small squares in the grid and the hydraulic conductivity of the domain. Flow-nets can easily be used for the evaluation of seepage underneath a dam, uplift forces on the dam, the effect of cut-off walls, etc.

4.3.3 Anisotropic Porous Medium

Expressions referring to flow through porous media in the preceding paragraphs consider the hydraulic conductivity as a scalar parameter and property. In cases of anisotropy of the domain, the hydraulic conductivity can be represented as a second-order tensor. As an example, in natural sandy soils, the

average hydraulic conductivity in a horizontal direction can be from two to ten times the value for the vertical direction. In cases of anisotropy of the porous medium, the last part of Eq. (4.3.10) is written as

$$K_H \frac{\partial^2 h}{\partial x^2} + K_V \frac{\partial^2 h}{\partial y^2} = 0 \tag{4.3.11}$$

where K_H and K_V are the horizontal and vertical hydraulic conductivity, respectively.

It is convenient to define a new coordinate x_1 by

$$x_1 = x\sqrt{\frac{K_V}{K_H}} \tag{4.3.12}$$

Introducing Eq. (4.3.12) into Eq. (4.3.11), the piezometric head again satisfies the Laplace equation. Therefore, a modification in the construction of the flow-net is necessary to allow consideration of domains with different horizontal and vertical hydraulic conductivity. This involves drawing the domain of reference and its boundary conditions with the horizontal dimensions reduced by the factor $\sqrt{K_V/K_H}$. Then the flow-net is drawn for the distorted boundaries and the discharge is computed using the average harmonic hydraulic conductivity,

$$K = \sqrt{K_H K_V} \tag{4.3.13}$$

4.3.4 Flow-Nets

Nowadays, quick solutions of the Laplace equation can be obtained by numerical approaches, which will be reviewed in subsequent chapters. However, it is appropriate to consider at this stage some particular examples of possible uses of flow-net construction. By these examples, some characteristics of flow through porous media can be visualized. For example, in the case of percolation under a dam through the porous layer of alluvial material which overlies an impervious layer, the flow pattern is independent of the upstream and downstream water levels. The difference, H, in these levels only determines the scale of the flow, as shown in Fig. 4.11. Since $\Delta\Phi$ is constant between adjacent equipotential lines, the total drop in piezometric head (equal to H) is divided along any flow line into increments, ΔH. Thus with n unit squares in each channel of the flow-net, the decrease in piezometric head, or uplift pressure head along the base of the dam, follows from the values of the piezometric head at the points of intersection of the equipotential lines with the base.

The effectiveness of cutoff walls and sheet piling in various locations and of upstream and downstream aprons in reducing uplift pressures can be evaluated by means of the flow-net. Each of these devices lengthens the seepage

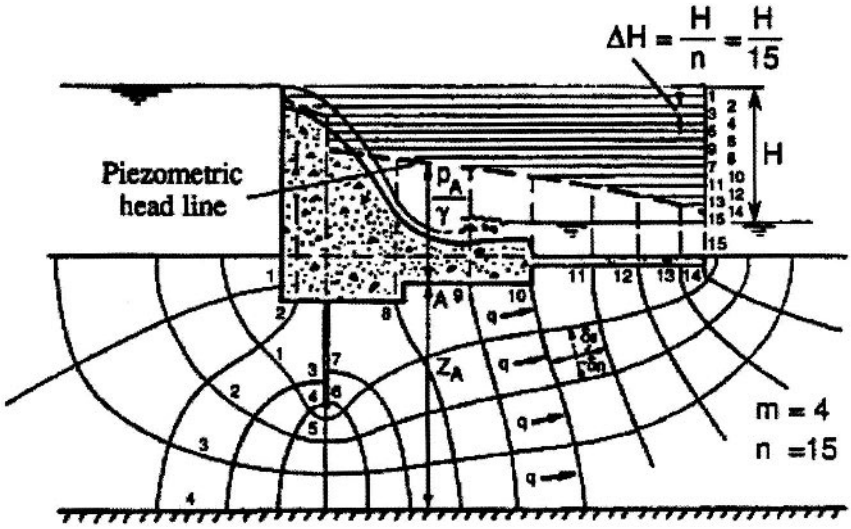

Figure 4.11 Flow-net under a dam.

paths, with cutoff walls producing a vertical drop in the piezometric head and aprons decreasing its gradient. Points of high velocity at the downstream end of the net, where "piping" may occur, can be identified and remedial measures can be evaluated.

The rate of flow through a unit square of one channel per meter width of the dam shown in Fig. 4.11 is

$$Q_s = -KA\frac{dh}{ds} = K\,\Delta n\frac{H/n}{\Delta s} = K\frac{H}{n} \tag{4.3.14}$$

where A is the cross-sectional area of a single channel, which is also the height of the small square of the flow-net, whose value is Δn. The length of the small square is Δs. The value of H is equally divided along the n lengths of the small squares. For m channels, each carrying an equal flow rate Q_s, the total flow-rate Q is mQ_s, or

$$Q = K\frac{m}{n}H \tag{4.3.15}$$

With regard to the total flow rate, the flow-net determines the ratio m/n. In its construction, the number of channels m is arbitrarily selected. The number of squares per channel varies with the number of channels, but the total flow-rate determinations for different values of m should agree with each other. The construction of the flow-net proceeds upstream and downstream

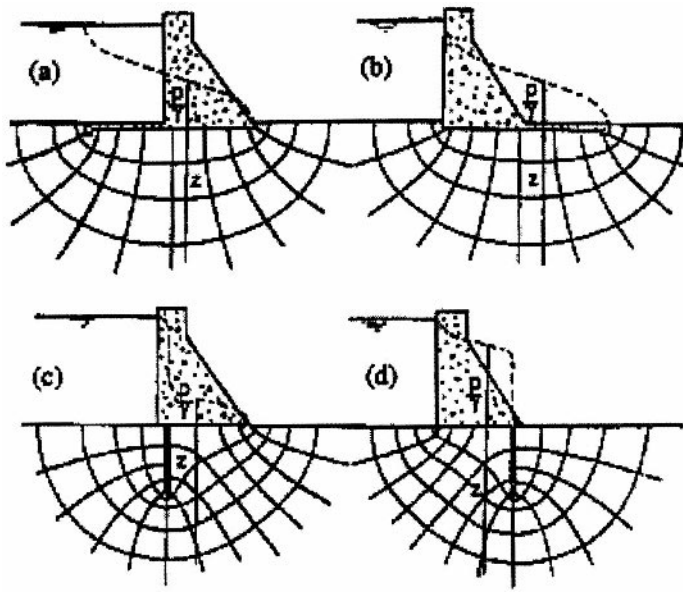

Figure 4.12 Possible effect of apron and cutoff wall on piezometric head distribution: (a) horizontal apron at head of dam; (b) apron at toe of dam; (c) vertical cut off wall near head of dam; and (d) vertical wall near toe of dam.

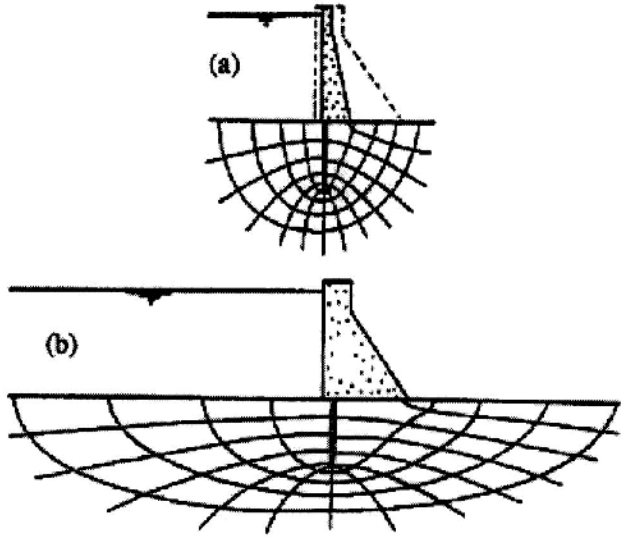

Figure 4.13 Flow net for anisotropic porous media.

from trial locations of the portions of the streamlines in the narrowest region of the flow path.

Figure 4.12 provides several examples concerning the possible effect of apron and cutoff wall on the distribution of the piezometric head in the alluvial layer. Figure 4.13 exemplifies use of the flow-net for anisotropic porous material.

4.4 CALCULATION OF FORCES

4.4.1 Force on a Cylinder

Figure 4.14 shows a cylinder of arbitrary cross section in a two-dimensional flow field. The fluid is assumed to be inviscid. The pressure force acting on an element of the surface is $p\,ds$ and it is normal to the surface element ds. The cylinder width, perpendicular to the paper plane of Fig. 4.14, is unity. The components of the pressure force in the x and y-directions are

$$\begin{aligned} F_x &= -p\,ds\cos\left(\theta - \frac{\pi}{2}\right) = -p\,ds\sin\theta = -p\,dy \\ F_y &= -p\,ds\sin\left(\theta - \frac{\pi}{2}\right) = p\,ds\cos\theta = p\,dx \end{aligned} \tag{4.4.1}$$

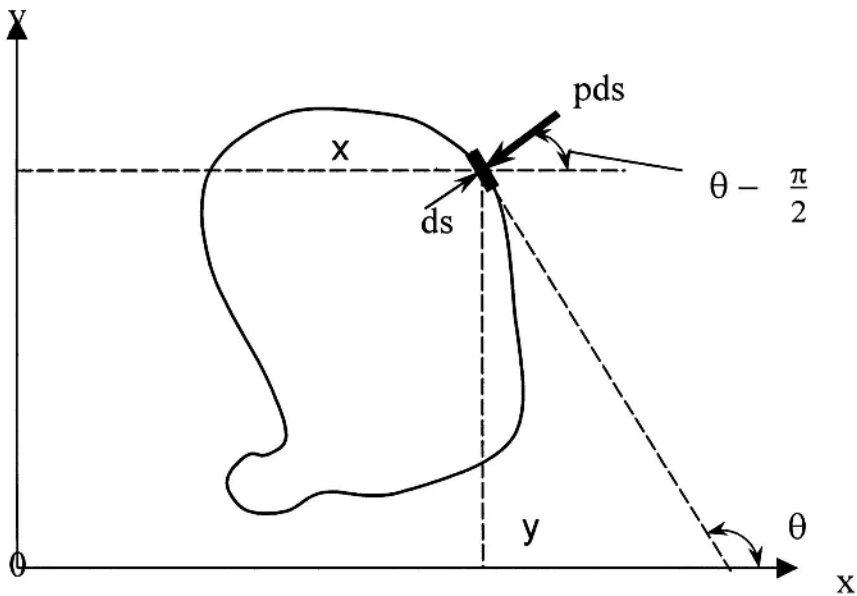

Figure 4.14 Pressure force acting on an elementary surface.

where θ is the angle made by the surface element with the x axis. The total pressure force components in the x- and y-directions are obtained by integrating over the cylinder surface,

$$F_x = \oint_c -p\,dy \qquad F_y = \oint_c p\,dx \tag{4.4.2}$$

4.4.2 Steady Flow Around a Circular Cylinder Without Circulation

Steady flow around a circular cylinder without circulation can be expressed as a superposition of uniform flow and a doublet, with velocity potential given by

$$w = U\left(z + \frac{a^2}{z}\right) = U\left[r\exp(i\theta) + \frac{a^2}{r}\exp(-i\theta)\right] \tag{4.4.3}$$

Following the procedures of Sec. 4.2, this complex potential is separated into the potential and stream functions,

$$\Phi = U\left(r + \frac{a^2}{r}\right)\cos\theta \qquad \Psi = U\left(r - \frac{a^2}{r}\right)\sin\theta \tag{4.4.4}$$

Figure 4.15 represents a schematic description of several streamlines of the flow around a cylinder without circulation.

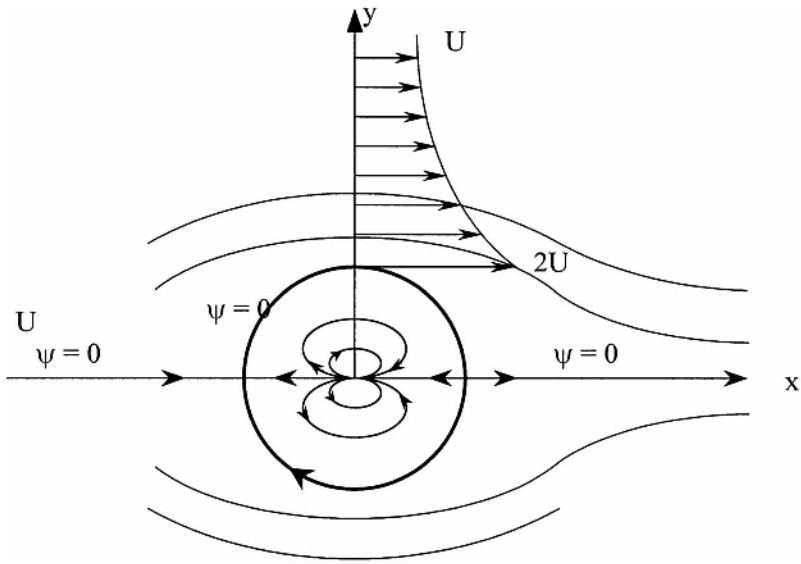

Figure 4.15 Steady flow around a cylinder without circulation.

The complex velocity for this flow field is

$$\frac{dw}{dz} = U\left(1 - \frac{a^2}{z^2}\right) = U\left[1 - \frac{a^2}{r^2}\exp(-i2\theta)\right] \tag{4.4.5}$$

This expression indicates that there are two stagnation points in the domain, defined by $r = a$ and $\theta = 0, \pi$. Then, according to Eq. (4.4.4), the stagnation points are located on the streamline defined by $\Psi = 0$. This line separates the fluid associated with the uniform flow from the fluid associated with the doublet and causes the flow field to behave as if there were a solid surface coincident with this streamline. According to Eq. (4.4.5), the absolute velocity along the separating streamline is

$$V^2 = \left|\frac{dw}{dz}\right|^2 = U^2\left[(1 - \cos 2\theta)^2 + (\sin 2\theta)^2\right] = 4U^2 \sin^2\theta \tag{4.4.6}$$

Figure 4.15 shows the velocity distribution along the y axis above the cylinder. According to Bernoulli's equation,

$$\frac{p_s}{\rho g} = \frac{p}{\rho g} + \frac{V^2}{2g} = \frac{p_\infty}{\rho g} + \frac{U^2}{2g} \tag{4.4.7}$$

where p_s is the pressure at the stagnation point and p_∞ is the pressure far from the cylinder. We now refer to the surface of the circular cylinder, $r = a$. The surface element for this cylinder is $ds = a\,d\theta$. Introducing this quantity, along with Eqs. (4.4.6) and (4.4.7) into Eq. (4.4.1), the pressure distribution is obtained along the surface as shown in Fig. 4.16. By integrating the pressure

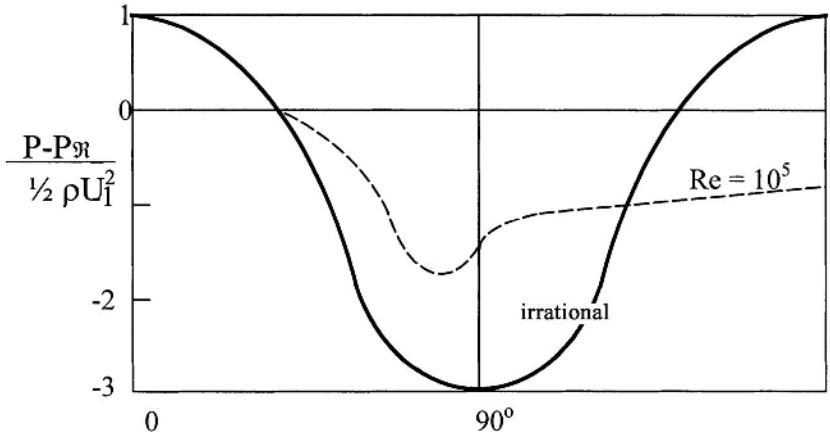

Figure 4.16 Pressure distribution around a cylinder without circulation.

distribution over the cylinder surface, it is easy to show that there is zero resultant force acting on the cylinder. This result indicates that according to potential flow theory, no drag or lift forces act on a body moving in a domain of inviscid fluid. This result is called *d'Alembert's paradox*. In real fluids there is always drag force acting on the body. The drag force originates from friction and separation of the flow from the sides of the body. The flow separation results in a wake and eddies migrating downstream of points of separation. The pressure at the wake is approximately equal to the pressure at the separation point, which is smaller than that predicted by potential flow theory. Therefore real fluid flow around the cylinder is always associated with drag force. A schematic description of the pressure distribution around the circular cylinder with a real fluid is shown in Fig. 4.16.

4.4.3 Steady Flow Around a Circular Cylinder with Circulation

In this case, a clockwise potential vortex with circulation Γ is added to the previous situation of a doublet in a uniform flow. The complex potential is now given by

$$w = U\left(z + \frac{a^2}{z}\right) + \frac{i\Gamma}{2\pi}\ln z \tag{4.4.8}$$

This expression can be separated to provide expressions for the potential and stream functions, and differentiated to yield an expression for the complex velocity, as before,

$$\begin{aligned} \Phi &= U\left(r + \frac{a^2}{r}\right)\cos\theta - \frac{\Gamma}{2\pi}\theta; \\ \Psi &= U\left(r - \frac{a^2}{r}\right)\sin\theta + \frac{\Gamma}{2\pi}\ln r \end{aligned} \tag{4.4.9}$$

$$\frac{dw}{dz} = U\left(1 - \frac{a^2}{z^2}\right) + \frac{i\Gamma}{2\pi z} \tag{4.4.10}$$

The streamline $\Psi = \Gamma/(2\pi)\ln a$ represents the circular cylinder $r = a$. Therefore the complex potential of Eq. (4.4.8) refers to uniform flow around a circular cylinder. At a large value of z, Eq. (4.4.10) indicates that the velocity is U. Referring to the surface of the circular cylinder, Eq. (4.4.10) yields the

value of the absolute velocity,

$$V = \left|\frac{dw}{dz}\right|_{r=a} = \left|\left[2U\sin\theta + \frac{\Gamma}{2\pi}\right](\sin\theta + i\cos\theta)\right| = \left|2U\sin\theta + \frac{\Gamma}{2\pi}\right| \tag{4.4.11}$$

This expression indicates that the velocity vanishes if

$$\sin\theta = -\frac{\Gamma}{4\pi aU} \tag{4.4.12}$$

Results of this expression are schematically represented by Fig. 4.17. There are two stagnation points if $\Gamma < 4\pi aU$. If $\Gamma = 4\pi aU$ then there is a single stagnation point at the cylinder surface. If $\Gamma > 4\pi aU$ then the stagnation point moves downward into the flow.

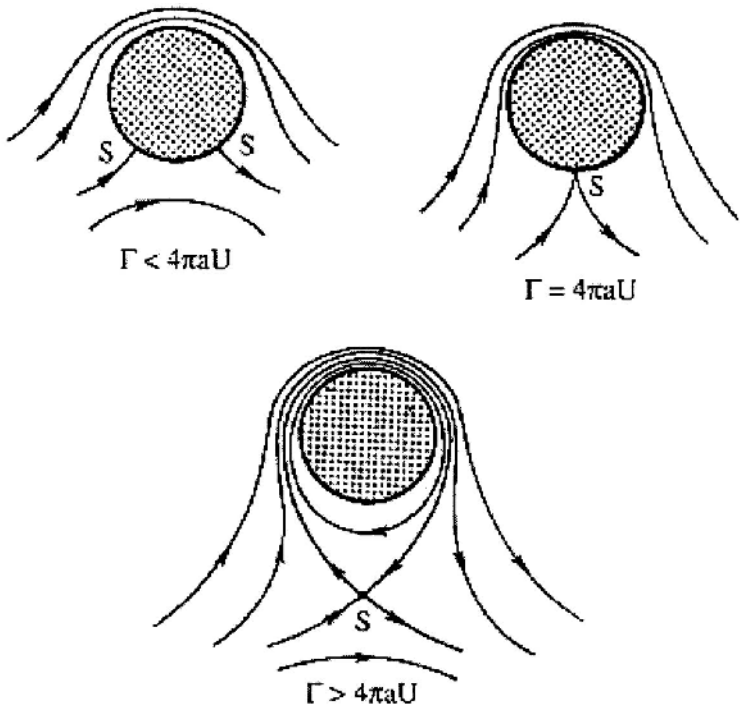

Figure 4.17 Flow around a cylinder with circulation.

The pressure distribution along the cylinder surface is again obtained by using the Bernoulli equation,

$$p + \frac{1}{2}\rho V^2 = p_\infty + \frac{1}{2}\rho U^2 \tag{4.4.13}$$

where p_∞ is the pressure far from the cylinder. Introducing Eq. (4.5.11) into Eq. (4.5.13), the pressure distribution on the cylinder surface is found to be

$$p_{r=a} = p_\infty + \frac{1}{2}\rho \left[U^2 - \left(2U \sin\theta + \frac{\Gamma}{2\pi a} \right)^2 \right] \tag{4.4.14}$$

The symmetry of the flow about the y axis indicates that there is no drag (net pressure force in the x-direction) for this flow field. On the other hand, the circulation leads to lift force (net pressure force applied on the cylinder in the y-direction). The calculation of the lift force is obtained by integration of Eq. (4.4.14),

$$F_y = -\int_0^{2\pi} p_{r=a} \sin\theta a \, d\theta = \rho U \Gamma \tag{4.4.15}$$

This expression is valid for potential flow around any two-dimensional body and is known as the *Kutta–Zhukhovski lift theorem*. This theorem is discussed further in Sec. 4.4.5.

In flow of real fluids around bodies, circulation is created due to the viscosity of the fluid. However, the magnitude of the circulation does not depend on the viscosity. Rather, it depends on the free flow velocity U and the shape of the body. In terms of potential flow theory, circulation around a circular cylinder can be created only by rotating the cylinder, around which fluid flows with a uniform flow velocity U.

4.4.4 The Theorem of Blasius

Equation (4.4.1) can be represented as a complex quantity,

$$dF_x - i\,dF_y = d\tilde{F} = -p\,dy - ip\,dx = -ip\,d\tilde{z} \tag{4.4.16}$$

where the wavy overbar denotes the complex conjugate. By integrating Eq. (4.4.16) over the entire surface of the cylinder, we obtain

$$F_x - iF_y = \tilde{F} = -i \oint_c p\,d\tilde{z} \tag{4.4.17}$$

where c denotes integration over the entire surface of the cylinder in the counter-clockwise direction.

By applying the Bernoulli equation between a reference point far from the cylinder and any other point in the flow domain,

$$p_\infty + \frac{1}{2}\rho U^2 = p + \frac{1}{2}\rho(u^2 + v^2) = p + \frac{1}{2}\rho(u + iv)(u - iv) \tag{4.4.18}$$

Introducing this expression for p into Eq. (4.4.16), we obtain

$$\tilde{F} = -i \oint \left[p_\infty + \frac{1}{2}\rho U^2 - \frac{1}{2}\rho(u + iv)(u - iv) \right] d\tilde{z} \tag{4.4.19}$$

The integral of $(p_\infty + \rho U^2/2)$ vanishes, as this term has a constant value. With regard to other terms of the integral in Eq. (4.4.19), first note that

$$\begin{aligned} u + iv &= V \exp(i\theta) \\ (u - iv)(u + iv)\, d\tilde{z} &= (u^2 + v^2)\, d\tilde{z} \end{aligned} \tag{4.4.20}$$

Introducing these expressions into Eq. (4.4.19), we obtain

$$\tilde{F} = i\frac{\rho}{2} \oint_c \left| \frac{dw}{dz} \right|^2 d\tilde{z} \tag{4.4.21}$$

This equation is called the *Blasius theorem*. It expresses the total pressure force applied on a cylinder of any shape that is submerged in a fluid subject to potential flow.

The Cauchy integral theorem states that the line integral of a complex function around any closed curve is zero, provided that no singular point is present in the region enclosed by the curve. If one or more singular points are present in that region, then the closed line integral does not vanish. The value of that integral does not depend on the closed curve chosen for the calculation of the integral, provided that the number of singular points in the enclosed region is kept constant. According to the theory of complex variables, the closed line integral around the singular points is equal to $2\pi i$ multiplied by the sum of the residues of all singular points in the enclosed region.

4.4.5 The Lift Theorem of Kutta–Zhukovski

According to the Blasius and Chauchy integral theorems, we may perform the integral of Eq. (4.4.21) at a large distance from the center of the cylinder, which can be represented by a superposition of uniform flow with sources, sinks, and doublets. From a large distance, all singular points are considered to be close to the origin. Therefore the complex potential function is given by

$$w = Uz + \frac{q}{2\pi}\ln z + \frac{i\Gamma}{2\pi}\ln z + \frac{\chi}{z} + \cdots \tag{4.4.22}$$

As the superposition refers to a closed curve representing the cylinder, the net flux of sources and sinks should be zero. Therefore by introducing Eq. (4.4.22) into Eq. (4.4.21) we obtain

$$\tilde{F} = i\frac{\rho}{2}\oint \left| U + \frac{i\Gamma}{2\pi z} - \frac{\chi}{z^2} + \cdots \right|^2 dz \tag{4.4.23}$$

The residue of the complex function subject to integration in Eq. (4.4.23) is the coefficient of the term incorporating 1/z in the power series expansion of that function. This coefficient is equal to $i\Gamma U/\pi$. Therefore Eq. (4.4.23) yields

$$\tilde{F} = i\frac{\rho}{2}\left[2\pi i\left(i\frac{\Gamma U}{\pi}\right)\right] = -i\rho U\Gamma \tag{4.4.24}$$

This expression indicates that the potential flow theory predicts that no drag force is applied on the cylinder, and the lift force is proportional to ρ, U, and Γ, as

$$F_x = 0 \qquad F_y = \rho U\Gamma \tag{4.4.25}$$

This result is called the Kutta–Zhukhovski lift theorem, as previously noted.

4.5 NUMERICAL SIMULATION CONSIDERATIONS

Numerical simulations of potential incompressible flows are based on the solution of the Laplace equation, in terms of the potential or the stream function,

$$\nabla^2\Phi = 0 \qquad \nabla^2\Psi = 0 \tag{4.5.1}$$

In a two-dimensional Cartesian coordinate system this equation for Φ is

$$\frac{\partial^2\Phi}{\partial x^2} + \frac{\partial^2\Phi}{\partial y^2} = 0 \tag{4.5.2}$$

This expression is a second-order partial differential equation (PDE). As discussed in Sec. 1.3.3, the order of a PDE is determined by the highest order derivative in the equation. Furthermore, Eq. (4.5.2) is a linear PDE. In a linear PDE, the coefficients of the highest order derivatives are constants or functions of the independent variables x and y.

The general format of a second-order linear PDE in a two-dimensional domain can be written as

$$a\frac{\partial^2\varphi}{\partial x^2} + b\frac{\partial^2\varphi}{\partial x\partial y} + c\frac{\partial^2\varphi}{\partial y^2} = f \tag{4.5.3}$$

where f represents a linear combination of coefficients multiplied by lower order derivatives of the dependent variable φ. The method and form of the solution of a PDE subject to initial and boundary conditions depend on the type of the PDE. As discussed in Chap. 1, it is common to classify a PDE according to the relationships between the coefficients of Eq. (4.5.3), as follows:

$$\text{If } b^2 - 4ac > 0 \text{ then the PDE is hyperbolic} \tag{4.5.4a}$$

$$\text{If } b^2 - 4ac = 0 \text{ then the PDE is parabolic} \tag{4.5.4b}$$

$$\text{If } b^2 - 4ac < 0 \text{ then the PDE is elliptic} \tag{4.5.4c}$$

According to Eq. (4.5.4), the Laplace Eq. (4.5.2) is an elliptic PDE.

For elliptic PDEs there are no initial conditions (note that time does not appear as an independent variable in Eq. 4.5.2), but only boundary conditions, which must be expressed in terms of some property of the dependent variable. For the present case, four boundary conditions are needed, two in each coordinate direction. In Eq. (4.5.2), Φ is the dependent variable. In the two-dimensional $x-y$ domain, any time-dependent phenomenon associated with the value of Φ is introduced, under unsteady-state conditions, through the boundary conditions. However, at this point we consider steady-state flows only. Because Eq. (4.5.2) is a second-order PDE with regard to x as well as with regard to y, there are three types of linear boundary conditions that can be applied to its solution (see also Sec. 1.3.3):

(1) All values of Φ are specified on the boundaries of the flow domain, or

$$\Phi = f(x, y) \quad \text{where} \quad (x, y) \in G \tag{4.5.5}$$

and G is the surface of the domain. With regard to the surface shown in Fig. 4.18 we may write

$$\begin{aligned} &\Phi = f_1(x, y_1) \qquad \Phi = f_2(x_2, y); \\ &\Phi = f_3(x, y_2) \qquad \Phi = f_4(x_1, y) \end{aligned} \tag{4.5.6}$$

so that the required four boundary conditions are provided. Boundary conditions of the type represented by Eqs. (4.5.5) and (4.5.6) are referred to as *Dirichlet boundary conditions*.

(2) All values of the gradient of Φ, i.e., the velocity components, are specified on the boundaries of the domain, so

$$\frac{\partial \Phi}{\partial n} = f(x, y) \qquad \text{where} \qquad (x, y) \in G \tag{4.5.7}$$

and n represents a coordinate normal to the boundary G, and pointing away from it. Boundary conditions of this type are called *Neumann boundary conditions*.

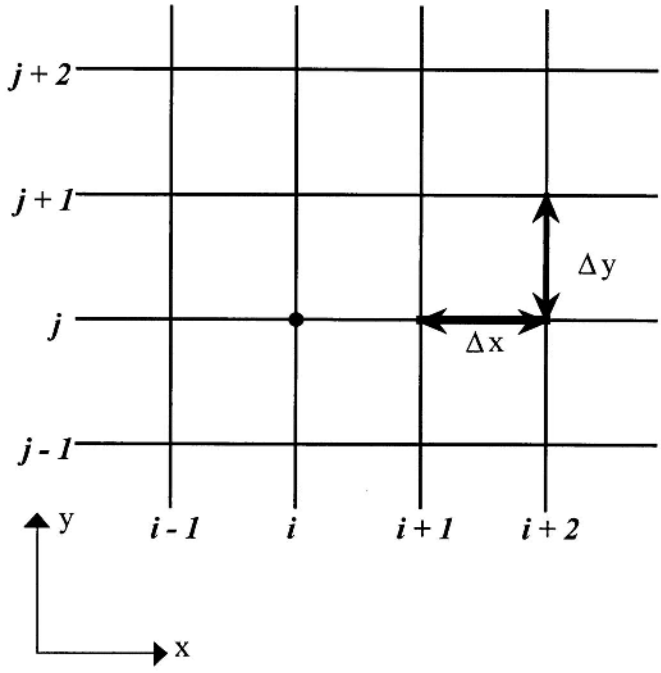

Figure 4.18 Example of a domain for an elliptic PDE.

(3) A general linear combination of Dirichlet and Neumann boundary conditions is written as

$$a\Phi + b\frac{\partial \Phi}{\partial n} = c \tag{4.5.8}$$

where a, b, and c are functions of position (x, y). Again, four such boundary conditions must be written.

Common linear boundary conditions are represented by solid boundaries. As previously noted, a solid boundary may be considered as a streamline. Therefore the velocity component perpendicular to the solid boundary vanishes. Complete analysis and simulation of a flow domain concerns the determination of the distribution of the velocity components and the pressure. Determination of the potential function Φ in the entire domain basically yields the velocity distribution. Then by using the Bernoulli equation, we obtain the pressure distribution. However, very often the pressure is the variable specified on some portions of the domain. As an example, consider the case of free

surface flow. For this type of flow the free surface is a streamline, on which the pressure vanishes. The given pressure provides a nonlinear specification of the velocity at the surface, through the Bernoulli equation. Furthermore, the location of the free surface may be one of the unknown variables, which must be determined as part of the overall solution to the problem. If there is a simultaneous flow of immiscible fluids, then the employment of potential flow theory can sometimes be considered. In such cases, the interface between adjacent fluid domains represents a boundary, on both sides of which the pressure and normal flow velocity are identical. Again, this represents a sort of nonlinear boundary condition, since the position of the interface may not be known. Topics of nonlinear boundary conditions are beyond the scope of the present text.

Singular points in a flow domain can sometimes be introduced by simple means, based on measurable parameters. Typical examples are sources and sinks. Sometimes combinations of source sheets are used to represent solid bodies immersed in the flow domain. By such a presentation, the streamline shape of the immersed body can be simulated with small amounts of computer resources, and limited requirements for boundary conditions. Vortices cannot be created in a numerical simulation unless they are artificially introduced. The common boundary conditions of solid boundaries do not produce singular points typical of vortices. Therefore numerical simulation with simple Dirichlet or Neumann boundary conditions cannot simulate lift forces. The introduction of artificial vortices or vortex sheets is commonly used for the simulation of lift forces.

In the framework of the present section, we provide a basic presentation of finite difference solutions of the Laplace equation or the *Poisson equation*, which is the nonhomogeneous form of the Laplace equation. Figure 4.19 represents a portion of the domain covered by a finite difference grid. The grid is made of small squares, with equal spacing Δx and Δy in the x- and y-directions, respectively. For each nodal point, subscript i refers to the number of the x interval and subscript j refers to the number of the y interval. The finite *central difference* (i.e., nodal values are used from both sides of the node at which the derivative is to be evaluated) approximations of the first- and second-order derivatives of Φ for the nodal point (i, j) are given as

$$\left(\frac{\partial \Phi}{\partial x}\right)_{i,j} \approx \frac{\Phi_{i+1/2,j} - \Phi_{i-1/2,j}}{\Delta x} \tag{4.5.9a}$$

$$\left(\frac{\partial \Phi}{\partial y}\right)_{i,j} \approx \frac{\Phi_{i,j+1/2} - \Phi_{i,j-1/2}}{\Delta y} \tag{4.5.9b}$$

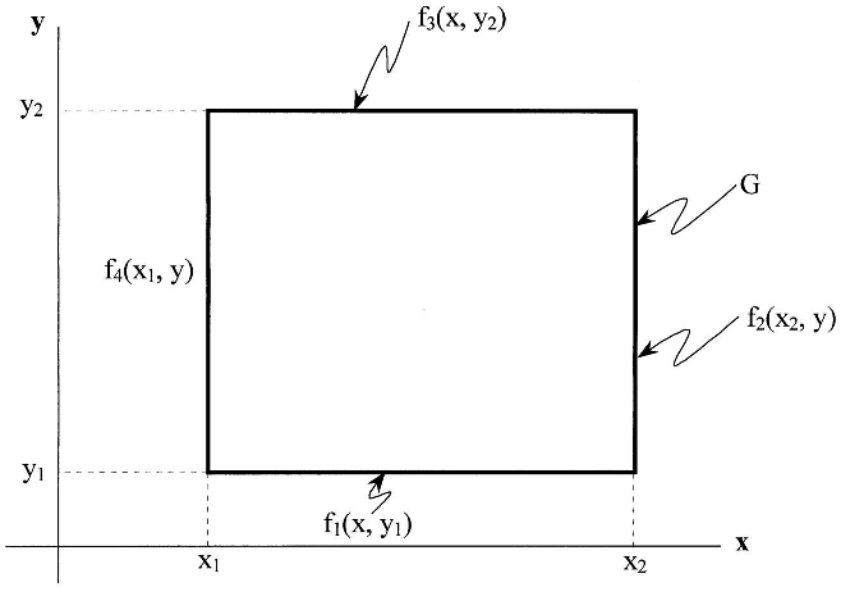

Figure 4.19 Portion of the domain covered by the finite difference grid.

$$\left(\frac{\partial^2 \Phi}{\partial x^2}\right)_{i,j} \approx \frac{1}{\Delta x}\left[\left(\frac{\partial \Phi}{\partial x}\right)_{i+1/2,j} - \left(\frac{\partial \Phi}{\partial x}\right)_{i-1/2,j}\right]$$
$$\approx \frac{\Phi_{i+1,j} - 2\Phi_{i,j} + \Phi_{i-1,j}}{(\Delta x)^2} \tag{4.5.10a}$$

$$\left(\frac{\partial^2 \Phi}{\partial y^2}\right)_{i,j} \approx \frac{1}{\Delta y}\left[\left(\frac{\partial \Phi}{\partial y}\right)_{i,j+1/2} - \left(\frac{\partial \Phi}{\partial y}\right)_{i,j-1/2}\right]$$
$$\approx \frac{\Phi_{i,j+1} - 2\Phi_{i,j} + \Phi_{i,j-1}}{(\Delta y)^2} \tag{4.5.10b}$$

As Eqs. (4.5.9) and (4.5.10) are obtained by a central difference approximation, their truncation error is of second order with respect to the grid interval. These representations also are valid when sources of strength q are located at some of the nodal points, in which case the Laplace equation is modified as the *Poisson equation*,

$$\frac{\Phi_{i+1,j} - 2\Phi_{i,j} + \Phi_{i-1,j}}{(\Delta x)^2} + \frac{\Phi_{i,j+1} - 2\Phi_{i,j} + \Phi_{i,j-1}}{(\Delta y)^2} = q_{i,j} \tag{4.5.11}$$

For convenience, since the numerical grid consists of small squares, it is assumed that $\Delta x = \Delta y = k$. Equation (4.5.11) then yields

$$\Phi_{i-1,j} + \Phi_{i+1,j} + \Phi_{i,j-1} + \Phi_{i,j+1} - 4\Phi_{i,j} = k^2 q_{i,j} \tag{4.5.12a}$$

$$\Phi_{i,j} = \frac{1}{4}(\Phi_{i+1,j} + \Phi_{i-1,j} + \Phi_{i,j+1} + \Phi_{i,j-1} - k^2 q_{i,j}) \tag{4.5.12b}$$

For simplicity, we assume there are no sources present in the domain, so that $q_{ij} = 0$ (i.e., solutions to the Laplace equation will be determined). Then, Eq. (4.5.12) indicates that the value of Φ at the i, j nodal point is the average of the four nodal points around that point. Each internal nodal point associated with subscripts $i < i_{\max} - 1$, and j not too close to the bottom and top boundaries of the domain shown in Fig. 4.5.3, leads to an equation with five unknown values of Φ, associated with the i, j point and the four nodal points around that point. Figure 4.20a illustrates a case in which Dirichlet boundary conditions are used. Figure 4.20b shows a case where Neumann boundary conditions are used.

Considering the case of Dirichlet boundary conditions, shown in Fig. 4.20a, grid points with subscript $i_{\max}$ are associated with a prescribed value of $\Phi = \Phi_1$. Therefore there is no need to use Eq. (4.5.12) for the determination of Φ at these boundary nodal points. For nodal points with subscript $i_{\max} - 1$, Eq. (4.5.12) incorporates the known value of $\Phi_{i\max,j}$. Therefore for the Laplace equation, only nodal points located in the proximity of the boundary have RHS values different from zero. A similar arrangement should be considered with regard to all other boundaries at which the value of the potential function is specified.

Considering the case of Neumann boundary conditions, shown in Fig. 4.20b, at grid points with subscript $i_{\max}$ the value of the derivative of Φ is given. The finite (central) difference approximation for that derivative can be represented by

$$\left(\frac{\partial \Phi}{\partial x}\right)_{i_{\max},j} = u_1 \approx \frac{\Phi_{i_{\max}+1,j} - \Phi_{i_{\max}-1,j}}{2\Delta x} \tag{4.5.13}$$

where the subscript $i_{\max} + 1$ represents an artifical extension of the numerical grid beyond the simulated flow domain. This is rearranged to solve for Φ at position $i_{\max} + 1$,

$$\Phi_{i_{\max}+1,j} = \Phi_{i_{\max}-1,j} + 2u_1 \Delta x \tag{4.5.14}$$

The linear equation set represented by Eq. (4.5.12) incorporates nodal points with subscript $i_{\max}$. The RHS of equations associated with these nodal

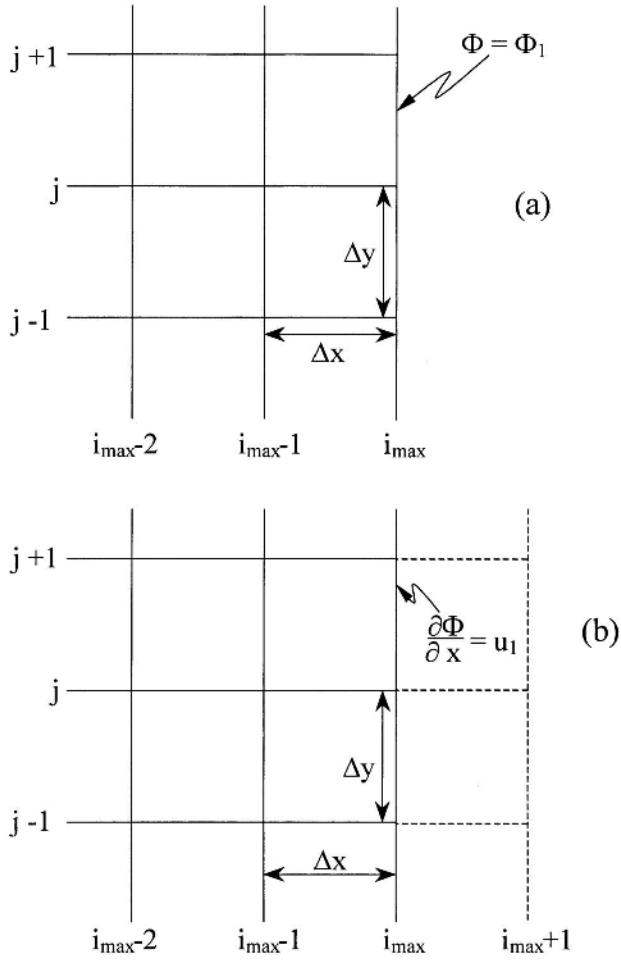

Figure 4.20 Numerical representation of boundary conditions: (a) Dirichlet boundary condition; and (b) Neumann boundary condition.

points is represented by a nonvanishing coefficient, provided that u_1 is different from zero. If $u_1 = 0$, then the line of i_{max} probably represents a solid boundary. In this case, nonvanishing RHS coefficients are provided at other boundaries of the domain. Expression similar to Eqs. (4.5.13) and (4.5.14) can be applied to all other boundaries of the flow domain at which the gradient of the potential function is specified.

The maximum number of unknown values of Φ incorporated in each nodal point in Eq. (4.5.12) is five. Therefore each row of the matrix of

coefficients of these unknowns includes a maximum number of five nonzero coefficients. The solution of the set of linear equations represented by Eq. (4.5.12) can be obtained using a noniterative method such as Gauss elimination. However, due to the large number of zero-valued coefficients in each row of the coefficient matrix, an iterative solution is more efficient than the noniterative approach in this case. The diagonal term in the coefficient matrix is the dominant term in each row of that matrix. Therefore convergence of the iterative procedure is guaranteed. In the following paragraphs, we present several common iterative procedures that can be applied to solve the set of linear equations represented by Eq. (4.5.12) when $q_{i,j} = 0$.

According to the iterative method of *Jacobi*, each new value of $\Phi_{i,j}$, at iteration $n + 1$, is obtained by using values of Φ, at nodal points around point (i, j), which were obtained at iteration n. Therefore, Jacobi's method implies that Eq. (4.5.12) should be modified as

$$\Phi_{i,j}^{(n+1)} = \frac{1}{4}\left[\Phi_{i-1,j}^{(n)} + \Phi_{i+1,j}^{(n)} + \Phi_{i,j-1}^{(n)} + \Phi_{i,j+1}^{(n)}\right] \tag{4.5.15}$$

where the superscript (in parentheses) indicates the iteration number at which the variable is calculated.

The method of *Gauss–Seidel* uses the latest computed values of Φ, as they become available during the iteration process. This method is slightly more efficient than that of Jacobi. The iteration algorithm for the solution of the Laplace equation by the Gauss–Seidel method is

$$\Phi_{i,j}^{(n+1)} = \frac{1}{4}\left[\Phi_{i-1,j}^{(n+1)} + \Phi_{i+1,j}^{(n)} + \Phi_{i,j-1}^{(n+1)} + \Phi_{i,j+1}^{(n)}\right] \tag{4.5.16}$$

The rate of convergence of the Gauss–Seidel method can be improved by using *successive over-relaxation* (SOR). According to this method, the provisional value Φ_p of the function Φ at the nodal point (i, j) and at iteration $(n + 1)$ is calculated by the Gauss–Seidel algorithm, but this value is modified at the $(n + 1)$ iteration by means of a *relaxation parameter* ω,

$$\Phi_{i,j}^{(n+1)} = \Phi_{i,j}^{(n)} + \omega\left[\Phi_p - \Phi_{i,j}^{(n)}\right] \tag{4.5.17}$$

where Φ_p is given by Eq. (4.5.16). If $\omega = 1$, then the SOR method is identical to the method of Gauss–Seidel. Equation (4.5.17) also can be written as

$$\Phi_{i,j}^{(n+1)} = \frac{\omega}{4}\left[\Phi_{i-1,j}^{(n+1)} + \Phi_{i+1,j}^{(n)} + \Phi_{i,j-1}^{(n+1)} + \Phi_{i,j+1}^{(n)}\right] + (1-\omega)\Phi_{i,j}^{(n)} \tag{4.5.18a}$$

or

$$\Phi_{i,j}^{(n+1)} = \Phi_{i,j}^{(n)} + \frac{\omega}{4}\left[\Phi_{i-1,j}^{(n+1)} + \Phi_{i+1,j}^{(n)} + \Phi_{i,j-1}^{(n+1)} + \Phi_{i,j+1}^{(n)} - 4\Phi_{i,j}^{(n)}\right] \tag{4.5.18b}$$

Finally, it should be noted that the solution of the Laplace or Poisson equation is based on an iterative solution of a set of linear equations, generally presented by

$$[A]\{\Phi\} = \{b\} \tag{4.5.19}$$

where $[A]$ is the matrix of coefficients of Φ values, $\{\Phi\}$ is the vector of Φ values, and $\{b\}$ is the vector of RHS coefficients of all the equations. There are many different ways to iterate and solve Eq. (4.5.19). The choice of the most appropriate method of solution depends mainly on convergence properties for a particular set of conditions.

PROBLEMS

Solved Problems

Problem 4.1 Confirm for each of the following flow fields that incompressible flow is indicated. Which of these represent potential flow? Why?

(a) $u = \alpha x \qquad v = -\alpha y$
(b) $u = \alpha y \qquad v = -\alpha x$
(c) $u = \alpha y \qquad v = \alpha x$
(d) $u_r = \dfrac{\alpha}{r} \qquad v = 0$

Solution

In a potential (and incompressible) flow, the following relationships should be satisfied:

$$\nabla \times \vec{V} = 0 \qquad \nabla \cdot \vec{V} = 0$$

In a Cartesian coordinate system, these expressions imply

$$\frac{\partial v}{\partial x} - \frac{\partial u}{\partial y} = 0 \qquad \frac{\partial u}{\partial x} + \frac{\partial v}{\partial y} = 0$$

In a plane polar coordinate system, these expressions yield

$$\frac{1}{r}\frac{\partial (r v_\theta)}{\partial r} - \frac{1}{r}\frac{\partial u_r}{\partial \theta} = 0 \qquad \frac{1}{r}\frac{\partial (r u_r)}{\partial r} + \frac{1}{r}\frac{\partial v_\theta}{\partial \theta} = 0$$

Upon considering each of the given velocity fields, by substituting into the above differential equations, we find

(a) Potential incompressible flow
(b) Rotational incompressible flow

(c) Potential incompressible flow
(d) Potential incompressible flow

Problem 4.2 Find the potential and stream functions, if possible, for each of the flows given in solved problem (4.1.1).

Solution

We apply Eqs. (4.2.5) and (4.2.6) to determine the expressions for the required functions:

(a) $$\Phi = \int u\,dx = \int \alpha x\,dx = \frac{\alpha x^2}{2} + f(y)$$

$$\frac{\partial \Phi}{\partial y} = f'(y) = v = -\alpha y; \quad \Rightarrow f(y) = -\frac{\alpha y^2}{2} + C;\ \text{assume } C = 0$$

$$\Phi = \frac{\alpha}{2}(x^2 - y^2)$$

$$\Psi = \int u\,dy = \int \alpha x\,dy = \alpha xy + f(x)$$

$$\frac{\partial \Psi}{\partial x} = \alpha y + f'(x) = -v = \alpha y \Rightarrow f'(x) = 0 \Rightarrow f(x) = C = 0$$

$$\Psi = \alpha xy$$

(b) Using the same approach as above, we obtain

$$\Psi = \frac{\alpha}{2}\left(x^2 + y^2\right)$$

Φ does not exist, since the flow is rotational

(c) $\Phi = \alpha xy \qquad \Psi = \dfrac{\alpha}{2}(y^2 - x^2)$

(d) $\Phi = \alpha \ln r = \dfrac{\alpha}{2}\ln(x^2 + y^2) \qquad \psi = \alpha\theta = \arctan\left(\dfrac{y}{x}\right)$

Problem 4.3 Determine the flow-net for the flow field created by the superposition of a uniform flow with speed U and a source of strength q, as shown in Fig. 4.21.

Solution

The complex potential is given by the sum of the potential functions for uniform flow and a source,

$$w = Uz + \frac{q}{2\pi}\ln z = Ur\cos\theta + \frac{q}{2\pi}\ln r + i\left(Ur\sin\theta + \frac{q}{2\pi}\theta\right)$$

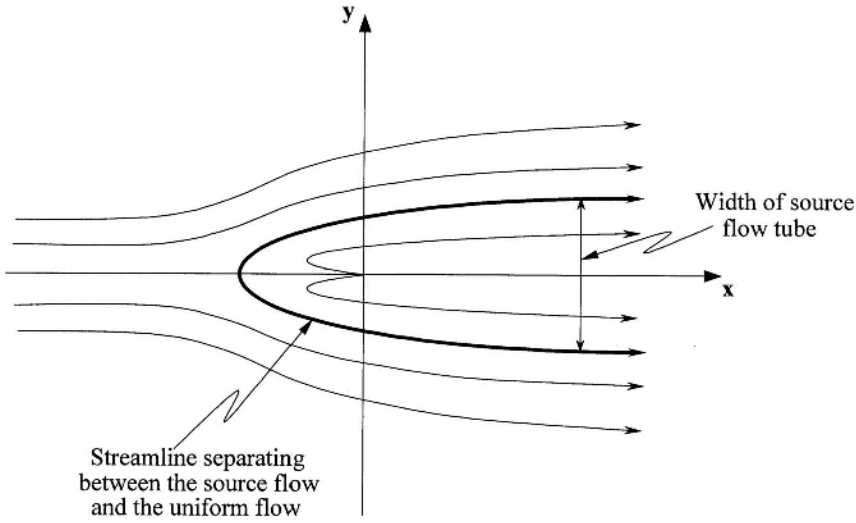

Figure 4.21 Superposition of source and uniform flow, Problem 4.3.

Therefore the potential and stream functions are

$$\Phi = Ur\cos\theta + \frac{q}{2\pi}\ln r \qquad \Psi = Ur\sin\theta + \frac{q}{2\pi}\theta$$

By differentiation of the complex potential, or either of the stream or potential functions, we obtain the following components of the velocity vector:

$$u_r = U\cos\theta + \frac{q}{2\pi r} \qquad v_\theta = -U\sin\theta$$

These expressions indicate that besides the cavitation singular point at $r = 0$, there is another singular stagnation point at $\theta = \pi$, $r = q/(2\pi U)$. We introduce the values of θ and r for the stagnation point into the expression of the stream function, to obtain the value of this function along the streamline, which separates the region between the uniform flow and the source flow. The result is

$$\Psi = \frac{q}{2}$$

Therefore, the streamline that separates the uniform flow from the source flow satisfies the following relationships:

$$r\sin\theta = \frac{q}{2U}\left(1 - \frac{\theta}{\pi}\right) \qquad \text{or} \qquad y = \frac{q}{2U}\left[1 - \frac{1}{\pi}\arctan\left(\frac{y}{x}\right)\right]$$

According to this expression, the width of the stream tube occupied by the source flow approaches the value $q/(2U)$ at a large distance from the origin.

Problem 4.4 If in Fig. 4.3.1, $H = 10$ m, and $K = 1$ m/day, provide an estimate of the seepage flow rate per one meter width of dam.

Solution

The solution to this problem is obtained by direct use of Eq. (4.3.15),

$$Q = K\frac{m}{n}H = 1 \times \frac{4}{15} \times 10 = 2.67 \text{ m}^3/(\text{day} \cdot \text{m}) \tag{4.3.16}$$

Problem 4.5 Water, with kinematic viscosity $v = 10^{-6}$ m^2/s, flows through sandy soil. The characteristic pore size of the soil is $d = 0.1 \times 10^{-3}$ m, and its porosity is $\phi = 0.3$.

(a) What are the permeability and hydraulic conductivity of the soil?
(b) Darcy's law is applicable up to a Reynolds number of one, where the Reynolds number is based on the characteristic pore size and the specific discharge. Determine the maximum value of the hydraulic gradient, for which Darcy's law can be applied.

Solution

(a) $$K = \frac{gd^2\phi}{32v} = \frac{9.81 \times (0.1 \times 10^{-3})^2 \times 0.3}{32 \times 10^{-6}}$$
$$= 9.2 \times 10^{-4} \text{ m/s} = 79.5 \text{ m/day}$$

(b) $$\text{Re} = \frac{qd}{v} = 1 \Rightarrow q = \text{Re}\frac{v}{d} = 1 \times \frac{10^{-6}}{0.1 \times 10^{-3}} = 10^{-2} \text{ m/s}$$
$$q = KJ \Rightarrow J = \frac{q}{K} = \frac{10^{-2}}{9.2 \times 10^{-4}} = 10.9$$

Unsolved Problems

Problem 4.6 Consider the Navier–Stokes equation for the x-direction (horizontal) velocity component (for simplicity, neglect rotation effects):

$$\frac{Du}{Dt} = -\frac{1}{\rho}\frac{\partial p}{\partial x} + v\nabla^2 u$$

where u is the velocity, p is pressure, ρ is density, and v is kinematic viscosity. For inviscid flow the viscosity is 0 and pressure is the only force to consider. Show that the viscous term also drops out, i.e., $\nabla^2 u = 0$, for the case of irrotational flow.

Problem 4.7 Consider the flow field created by a superposition of a source with strength q and a simple vortex, whose circulation Γ has the same magnitude as q.

(a) Find the complex potential, potential, and stream functions.
(b) Plot the flow-net.
(c) Find the pressure distribution along a radial coordinate.

Problem 4.8 Consider the flow field created by a superposition of a uniform flow with speed U, in the positive x-direction, a positive source, of strength q, located at $x = -a$, and a negative source (sink), located at $x = a$.

(a) Find the complex potential, potential, and stream functions.
(b) Find the location and types of singular points.
(c) Plot the flow-net.
(d) Find the pressure distribution along the x axis.

Problem 4.9 A simple vortex, with circulation Γ, is located at $x = a$, $y = b$, which is in a 90° corner between two solid walls. Determine the pathline of the vortex movement.

Problem 4.10 A flow field is created by two sources at a solid wall, which is represented by the y axis. One source, of strength q, is located at $x = a$. The second source, of strength $q/2$, is located at $x = 2a$.

(a) Find the complex potential, potential, and stream functions.
(b) Determine the locations and types of singular points.
(c) Plot the flow-net.
(d) Find the pressure distribution along the x axis.

Problem 4.11 Consider the flow domain represented by

$$z = a\cos(w)$$

where

$$z = x + iy \qquad w = \Phi + i\Psi$$

(a) Find the complex potential, potential, and stream functions.
(b) Determine the locations and types of singular points.
(c) Plot the flow-net.
(d) Find the pressure distribution along the x axis.

Problem 4.12 Wind blowing over a bluff is to be simulated using potential flow theory. A uniform wind, $U = 20$ m/s, is combined with a source, having a

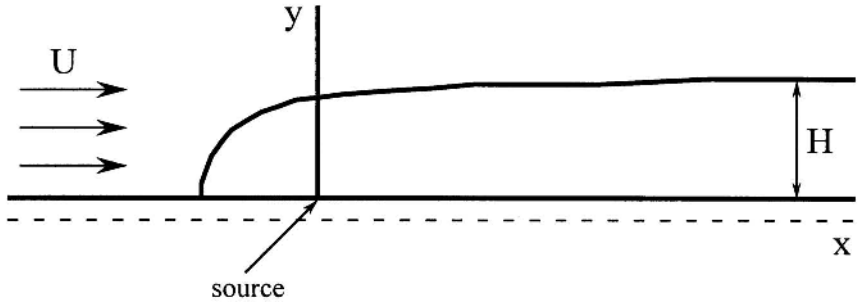

Figure 4.22 Simulation of flow over a buffer, Problem 4.12.

flow rate $q = 6{,}000\ \text{m}^2/\text{s}$. The resulting flow is sketched in Fig. 4.22 (only the top half of the bounding streamline is shown). Note that the stream function is

$$\Psi = Ur\sin\theta + m\theta$$

where m is $q/(2\pi)$.

(a) What is the equation for the bounding streamline?
(b) How high is the bluff (H)?
(c) What is the velocity along the surface of the bluff, directly above the source?

Problem 4.13 Flow over a hump is to be analyzed using potential flow theory. The mathematical expression for the flow field is developed by considering one-half of the field created by superimposing a doublet in a uniform flow. As shown in Fig. 4.23, the flow far from the hump has velocity U and

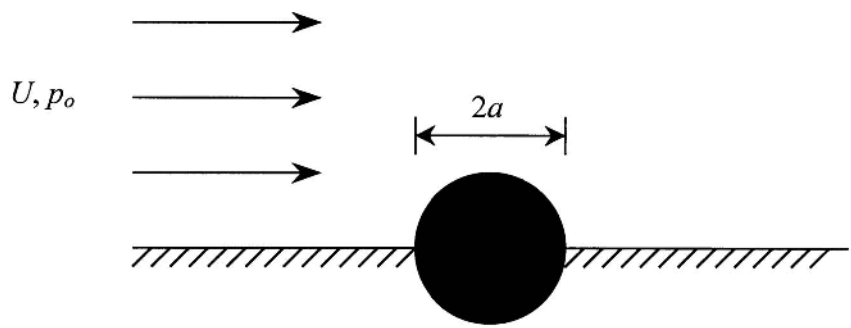

Figure 4.23 Definition sketch, Problem 4.13.

pressure p_o. The fluid density is ρ and it is incompressible. The streamline corresponding with the solid surface has $\Psi = 0$, and gravity effects may be neglected.

(a) What are the maximum and minimum pressures for this flow, in terms of ρ, U, and p_o?
(b) Develop the equation for the streamline passing through the point $r = 2a, \theta = \pi/2$.

Problem 4.14 Consider some possible values of the Rossby number in practical cases that you may encounter with regard to environmental flows in lakes and reservoirs. Choose real values for at least three examples.

Problem 4.15 The engineer of a municipality has suggested that a treated effluent can be disposed of by pumping it into an injection well. The well should be able to accept a flow of 500 m^3/h. It is drilled in an aquifer whose thickness is 40 m and hydraulic conductivity is 100 m/day. Upstream of the planned injection well, the municipality pumps its water supply needs from a pumping well with a capacity of 600 m^3/h. The natural flow in the aquifer is achieved with a gradient of 0.1%.

(a) Consider several hypothetical cases in which the effluent could possibly arrive at the pumping well. In other words, under what circumstances could this occur?
(b) Consider several possible values of the distance between the pumping and injection wells, and provide suggestions to the municipality on how migration of the effluent into the pumping well could be avoided.

Problem 4.16 Water flows through a confined aquifer of thickness 20 m. The hydraulic gradient is 0.1%, the hydraulic conductivity is 50 m/day, and the porosity is 0.3. The characteristic particle size of the aquifer sediment is 0.1 mm.

(a) Determine the specific discharge.
(b) Find the flow velocity.
(c) What is the Reynolds number of the flow?

Problem 4.17 Consider the schematics of flow under a concrete dam, as shown in Fig. 4.24. Depict the flow-net and provide an estimate of the total flow underneath the dam.

Problem 4.18 A function, which in the neighborhood of $z = a$ has an expansion that contains negative powers of $(z - a)$, is singular at $z = a$. In this case

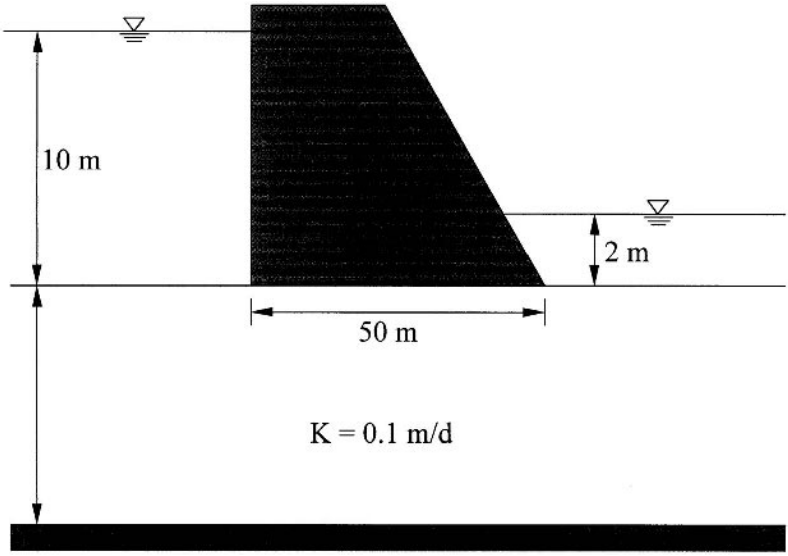

Figure 4.24 Definition sketch, Problem 4.17.

the coefficient of $(z-a)^{-1}$ is called the *residue* of the function at $z=a$. Determine the residue of the following functions:

(a) $(z-a)^n$ where $n=-1, 1, 2\ldots$

(b) $A_2(z-a)^2 + A_1(z-a) + A_0 + \dfrac{B_1}{(z-a)} + \dfrac{B_2}{(z-a)^2}$

Problem 4.19 According to *Cauchy's residue theorem*, the integral along a closed line C of a holomorphic function (a function of z) is given by

$$\oint_c f(z)\,dz = 2\pi i(a_1 + a_2 + a_3 + \cdots)$$

where $a_1, a_2, \ldots$ are the residues at the singular points of the area enclosed by the line C. Find the poles and corresponding residues of the following functions, as well as the integral of Chauchy's residue theorem:

(a) $\dfrac{z}{z+1}$ (b) $\dfrac{z+2}{z^2-1}$ (c) $\dfrac{z+z^2}{z^2+1}$ (d) $\dfrac{4z^2}{z^4-1}$

Problem 4.20 A source of strength q is placed at a point $(a, 0)$ outside the circle $|z| = b$, as shown in Fig. 4.25.

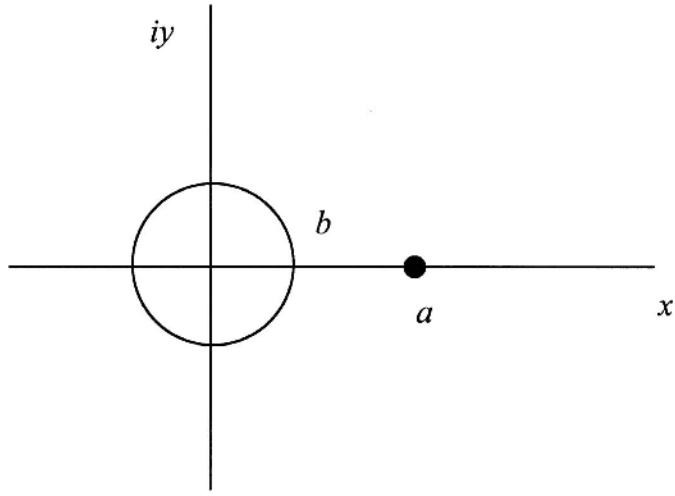

Figure 4.25 Definition sketch, Problem 4.20.

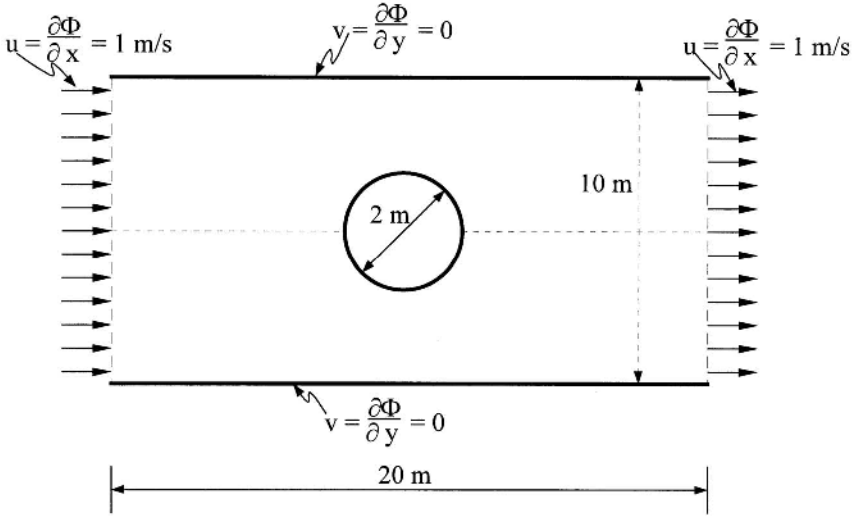

Figure 4.26 Bounded flow past a cylinder, Problem 4.21.

(a) Show that the complex potential describing the flow field is given by

$$w = \frac{q}{2\pi}\left[\ln(z-a) + \ln\left(z - \frac{b^2}{a}\right) - \ln z\right]$$

(b) Use the theorem of Blasius to prove that there is no moment about the center of the circle, and that the circle is urged towards the source by a force equal to

$$\frac{2\rho q^2 b^2}{\pi a(a^2 - b^2)}$$

(c) Find the corresponding result when the source is replaced by a vortex.

Problem 4.21 Consider the bounded potential flow around a cylinder as shown in Fig. 4.26. Provide a numerical solution and sketch the flow-net. Compare your results with the analytical solution for an infinite flow field.

SUPPLEMENTAL READING

Milne-Thomson, L. M., 1966. *Theoretical Aerodynamics*, Macmillan, London. (Contains a thorough coverage of all aspects of inviscid flow theory and applications.)

Wendt, J. F., ed. 1996. *Computational Fluid Dynamics*, Springer-Verlag, Berlin, Germany. (Includes a review of various approaches of numerical simulation of potential flows.)